JPRS-JST-92-024
29 SEPTEMBER 1992

JPRS Report

Science & Technology

Japan

12th High Tech Forum-Tribological Advances In Ceramics

Science & Technology

Japan

12th High Tech Forum - Tribological Advances In Ceramics

JPRS-JST-92-024 *29 September 1992*

CONTENTS

Triboemission of Ceramics

926C0070A Tokyo DAI 12-KAI SENTAN GIJUTSU FORAMU in Japanese 14 Feb 92 pp 1-5

[Article by K. Nakayama, Mechanical Engineering Laboratory]

[Text]

1. Introduction

The phenomenon whereby electrons, ions, photons and neutral particles are emitted through so-called tribological surface damage by friction is called triboemission[1)-6)]. Recent research has made it clear that this phenomenon is liable to occur in insulating materials, such as ceramics. This phenomenon seems to be deeply related to micro surface ruptures, micro electro phenomena and the tribochemical reaction of ceramics. This article will describe the characteristics and mechanism of this phenomenon, focusing on the recent research results obtained by the author, et al.

2. Change with Time

Figure 1 [not reproduced] illustrates a triboemission measuring device capable of the simultaneous measuring of positively and negatively charged particles, photons and friction coefficients in a vacuum, the atmosphere and various gaseous atmospheres[4),6)]. The principle involves scratching the surface of a rotating specimen with an insulating diamond stylus and measuring the charged particles and photons emitted through surface damage by scratching. For collecting charged particles when detecting them, voltages of -15 and +15 V are applied between the detector and the friction surface. Photons were detected by a PMT [photo multiplier tube]. This article's descriptions will focus on the data obtained by this device.

Figure 2 [not reproduced] shows the time dependence of the emission intensity of the charged particles, emission intensity and friction coefficient of photons when Al_2O_3 is scratched with a diamond indenter in the atmosphere[4)]. It is typical of triboemission from insulating substances, such as ceramics, that the particle emission of electrons, ions and photons occurs simultaneously and explosively as frictional damage starts, and stops simultaneously as the damage stops. This phenomenon is in symmetry with the fact that if there is some damage to the conductor metal surface, and even if scratching has ceased, the after emission continues[8)]. The emission intensity in Figure 2 is measured as the charge amount per 6 ms.

3. Material Dependence

The triboemission phenomenon is deeply related to the electric insulating quality of solids. particles are emitted less intensely from metals and more intensely from insulating substances in the atmosphere, with the emission intensity increasing in ascending order of conductors, semiconductors and insulators (Figure 3, [not reproduced])[4),6)]. Materials expected to be sliding materials, such as ceramics and polymers, and new materials are mainly insulating, which makes them liable to cause triboemissions.

On the other hand, although friction is a measure of energy consumption, what is the relationship between friction and triboemissions? When the same material is scratched, an increase in friction means an increase in nascent surfaces and triboemission intensity. When Al_2O_3 is scratched in the atmosphere with diamond tips of various shapes, the surface damage increases as the diamond tip sharpens, thereby resulting in an increase in friction and the emission of positively and negatively charged particles (Figure 4 [not reproduced])[3)]. This is because, as will be stated later, triboemission is related to the production of nascent surfaces by ruptures. As can be seen in Figure 3, however, there is no correlation between the friction coefficient and emission intensity. This is because, while friction is a function of two parameters, i.e., shearing strength and the hardness of a material, the production of a nascent surface related to triboemissions has something to do only with material hardness. In reality, the harder a material is, the more difficult it is for the surface to rupture and there is a reduction in the quantity of high energy nascent surfaces being generated; thus particle emissions generally decrease as hardness increases (Figure 5)[4),6)].

Let us examine the emission ratios of positively and negatively charged particles and the relationship between charged particles and photons. Figure 6 shows I^-/I^+, the negative-to-positive charged particle emission intensity ratios from the surfaces of various materials scratched in the atmosphere[4),6)]. In the atmosphere, negatively charged particles are mainly detected in conductors and semiconductors. On the other hand, both can be detected in insulators, although the emission intensity of negatively charged particles is slightly greater. As for photons, while no emissions from metals are observed, emissions from insulators and semiconductors follow without fail, demonstrating a good correlation between the two (Figure 7)[6)]. Thus, it is found that the emission mechanism of insulators differs from that of conductors.

It is very interesting that since SiC, a semiconductor, belongs to an insulator group in Figures 5 and 7 and to a conductor group in Figure 6, it is likely to have the emission mechanisms of both.

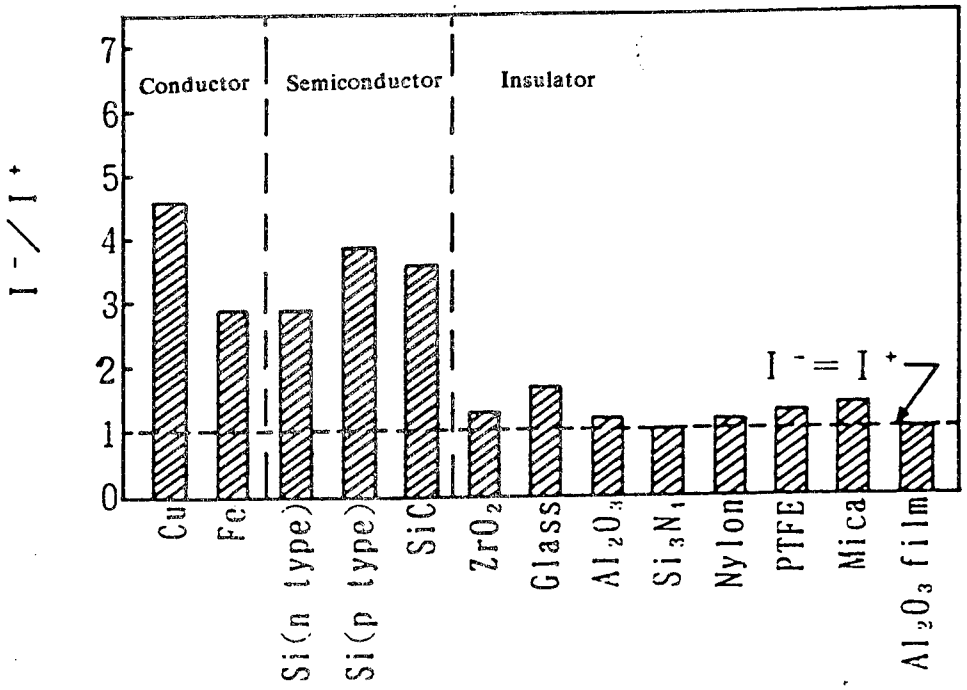

Figure 5. Relationship Between Emission Intensity and Hardness of Negatively-Charged Particles (in Air)

4. Emission Characteristics of Coating Materials

Furthermore, it can be observed in Figure 5 that Si_3N_4 provides fewer emissions of charged particles than does ZrO_2, although they are the same in hardness, thus suggesting the involvement of micro surface rupture characteristics, e.g., toughness. In reality, with aluminum anode oxide films, it has been observed that triboemission occurs following scratching as a result of the shapes of countless microcracks and crack generation (Figure 8 [not reproduced]), with the oxide film thickness influencing the microcrack shapes and crack density and the oxide film tissue influencing the triboemission[4]. With anode oxide films with parallel tissues, scratching at right angles to the tissue causes multiple cracks to be generated, followed by intense triboemission. Scratching parallel to the tissue causes a small number of cracks to be generated, followed by less intense triboemission. Therefore, such anode oxide films result in waves with the half revolution cycles of a disk (Figure 9 [not reproduced])[4]. As for anode oxide films with no tissue, no such emission waves can be observed. Thus, it is found that triboemission accompanies crack development.

5. Emission Mechanism

In their research on the behavior of exo-electron emission (PSEE) following the tensile deformation of Al anode oxide films, Sujak, et al., observed that an electric field is generated in the interior of cracks due to charge separation, calculating its value to be 6.8×10^5 V/cm, and concluding that the value was 10^7 V/cm in general[9]. Sujak's group noticed that this electric field value was sufficient to allow electrons to be emitted from the wall surfaces of cracks by field emission without light energization, explaining that the electrons are being emitted by field emission not from the bottoms of cracks, but from the wall surfaces of the anode oxide films themselves[10]. As stated above, along with the development of cracks following Al_2O_3 friction, not only the emission of positively and negatively charged particles, but also that of photons is observed. The charge separation discussed by Sujak, et al., may also have been produced in the wall surfaces of developing nascent cracks. In the atmosphere, as shown in Figure 11, gas (air in this case) molecules will be ionized before the field emission of electrons occurs. In reality, as shown in Figure 11, the emission intensity of positive and negative particles depends on the type of gas[4),7)]. The area resulting from charge separation can be proportional to the thickness of an oxide film and, as shown in Figure 12 [not reproduced], the emission intensity of positive and negative particles increases in proportion to the thickness of the oxide film[3]. These results suggest that triboemission is caused by the electrolytic dissociation of a gas in a friction surface.

However, while a gas does not necessarily undergo electrolytic dissociation when the gas ionization potential V_i has been exceeded, there is a certain probability

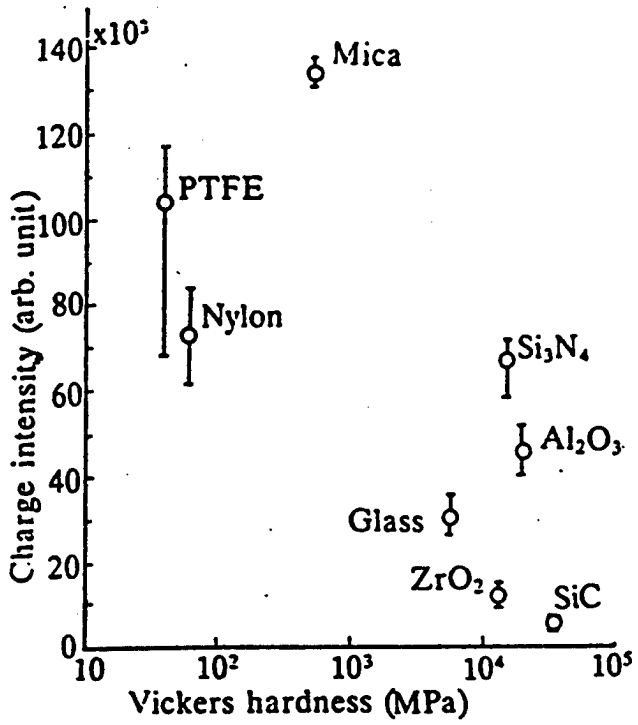

Figure 6. I^-/I^+, Ratio of Emission Intensity of Negatively-Charged Particles to Emission Intensity of Positively-Charged Particles (in Air)

(ionization probability) b that it will$_3$. It has been understood that no correlation exists between the charged particle emission intensity under atmospheric pressure and b in the neighborhood of this ionization potential, and that ionization of the main gas does not occur in the neighborhood of the first ionization potential[4),7)]. On the other hand, the spark discharge of gas molecules occurs in high electric fields. With photons being observed simultaneously, as shown in Figure 2 [not reproduced], it is well conceivable that this spark discharge occurs in a friction surface. V_s, the voltage generated by spark discharge, is a function of pl, the product of ambient gas pressure p and crack width (interelectrode distance) l, and, as is shown in Figure 13, the minimum value for $(pl)_m$, a certain value of pl, demonstrates that, whether that value is large or small, the V_s increases (Paschen's law). Table 1 shows crack wall surface voltage V_s, crack width l_c and in-crack field strength E found under the assumption that spark discharge occurs at thie minimum point[4),7)]. Table 1 also shows the impact ionization coefficient α by electrons of the gas molecules in the spark discharge calculated using these values. The field strength of 10^4 - 10^5 V/cm generated by the spark discharge in the friction surface given in Table 1 is smaller by two orders of magnitude than the field strength of 10^6-10^7 V/cm generated in the crack surface calculated by Sujak and his group, and, with cracks with gap lengths of the micrometer order occurring in friction surfaces, it is suggested that spark discharge is likely to occur in friction surfaces. In reality, it has been found that a linear relationship exists between the charged particle emission intensity and the α thus obtained, therefore concluding that triboemission is caused by the spark discharge of a gas in friction surfaces (Figure 13)[4),7)].

Table 1. Minimum Spark Discharge Voltage V_s, Crack Gap Length l_c, Field Strength E and Impact Ionization Coefficient α under Atmospheric Pressure

Gas	V_S (V)	l_C (μm)	E (V/cm)	α at 760 Torr
He	150	32.9	4.5×10^4	1,193
Ar	265	19.7	13×10^4	2,614
N_2	275	9.9	28×10^4	3,724
O_2	450	9.2	49×10^4	—
Air	330	7.5	44×10^4	5,905

In Figure 13, the emission intensity of negatively-charged particles is greater than that of positively-charged particles, which does not mean that negative

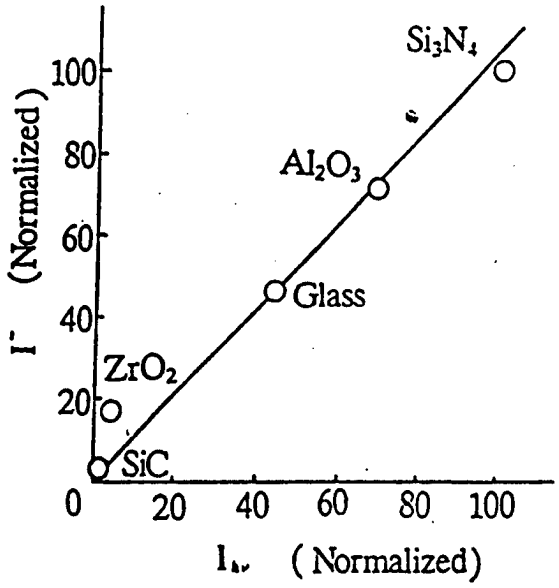

Figure 7. Relationship Between I^-, Emission Intensity of Negatively-Charged Particles, and I_{hv}, Emission Intensity of Photons (in Air)

particles generate more in friction surfaces. The same number of positively- and negatively-charged particles are generated by gas discharge in wear surfaces, but the difference in the migration rate for the distance from the friction surfaces to the detector causes the difference in detection results. This is confirmed by the fact that I^-/I^+, the detection strength ratio of the two, is virtually equivalent to μ^-/μ^+, the ratio of negative ion mobility to positive ion mobility [Table 2].

Table 2. Negative, Positive Ion Mobility μ^-, μ^+ ((cm/sec)/(V/cm)), μ^-/μ^+, I^-/I^+

Gas	μ^-	μ^+	μ^-/μ^+	I^-/I^+
He	6.32	5.14	1.23	1.59
Ar	1.71	1.32	1.30	1.45
N_2	1.84	1.28	1.44	1.79
O_2	1.84	1.32	1.20	
Air	2.11	1.32	1.59	1.72

Such triboemission has also been observed in a hydrocarbon atmosphere and, further, that of photons has been observed in hydrocarbon oil. Therefore, it is well conceivable that tribochemical reactions by these active particles are induced in oil lubrication.

6. Conclusion

The characteristics and mechanisms of triboemission have been discussed, and [it is concluded that] such active particle emissions are likely to influence ambient molecules. Therefore, it is probable that this phenomenon relates to various tribology phenomena through tribochemical reactions. It would be the author's pleasure if the results of triboemission phenomena stated here would aid in solving the tribology-related problems of ceramics.

References

1) Nakayama, K., Hashimoto, H., NORDTRIB '90 PROCEEDINGS, Technical University of Denmark, Dk-2800 Lyngby, Denmark, p 249; and also WEAR, Vol 147, 1991 p 335.

2) Nakayama, K., Suzuki, Y., Inaba, F., PREPRINTS OF THE TRIBOLOGY CONFERENCE, JAPAN LUBRICATION SOCIETY, Tokyo, 1990, p 297.

3) Nakayama, K., Hashimoto, H., PROC JPN INT TRIBOL CONF, Nagoya, Japanese Society of Tribologists, Tokyo, 1989, p 1141.

4) Nakayama, K., Hashimoto, H., PREPRINTS OF THE TRIBOLOGY CONFERENCE, JAPAN LUBRICATION SOCIETY, Tokyo, 1991, p 431.

5) Nakayama, K., Hashimoto, H., PREPRINTS OF THE TRIBOLOGY CONFERENCE, JAPAN LUBRICATION SOCIETY, Tokyo, 1991, p 435.

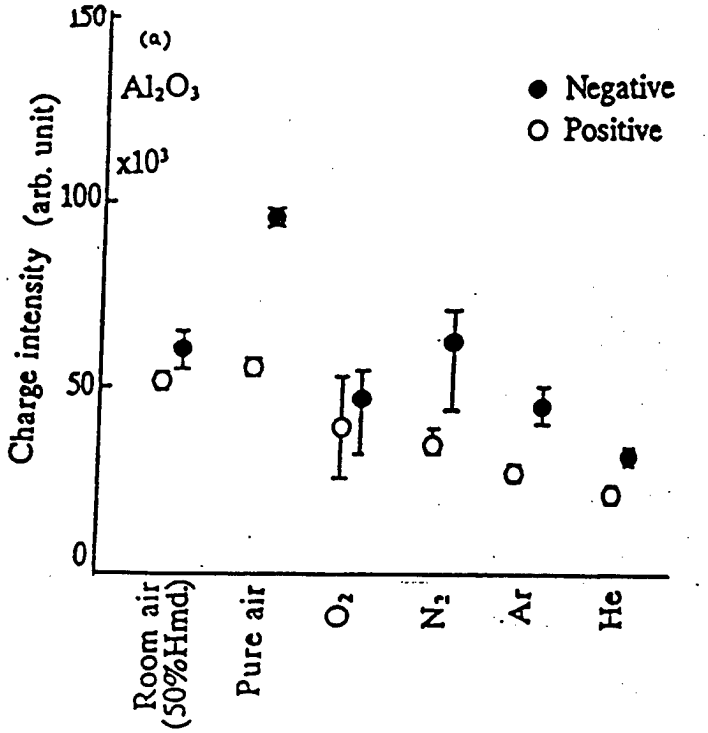

Figure 11. Emission Intensity (a) and Friction Coefficient (b) of Positively- and Negatively-Charged Particles in Various Gases

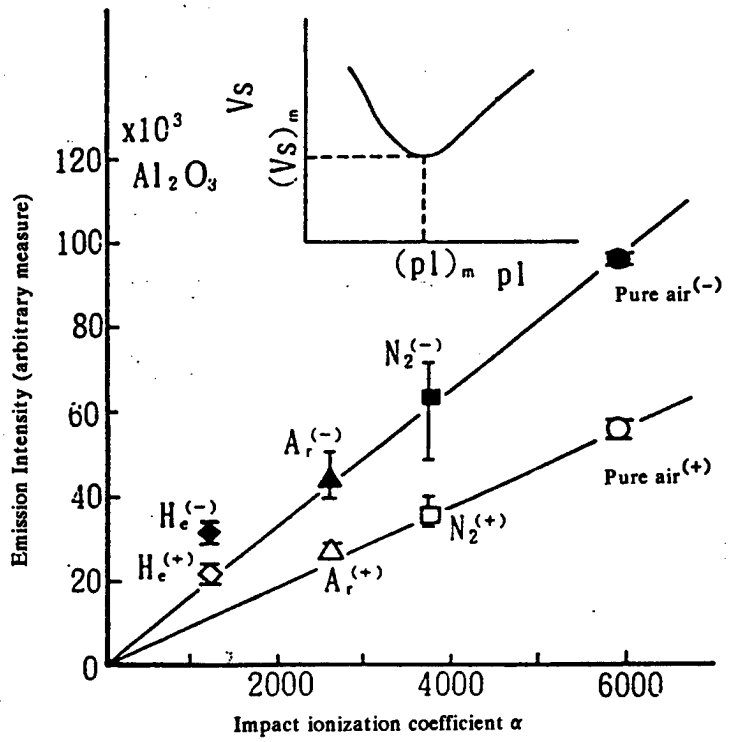

Figure 13. Relationship Between Emission Intensity and Impact Ionization Coefficient α of Charged Particles

6) Nakayama, K., Hashimoto, H., J PHYS D, APPL PHYS, in press.

7) Nakayama, K., Hashimoto, H., STLE Paper No 91-Tc-1D-4, will also appear in TRIBOLOGY TRANSACTIONS.

8) Nakayama, K., Leiva, J.A., Enomoto, Y., PREPRINTS OF THE 34TH NATIONAL CONFERENCE, JAPAN LUBRICATION SOCIETY (Toyama), 1989, p 329.

9) Sujak, B., Gieroszybski, A., Gieroszinska, K., ACTA PHYSICA POLONICA, Vol A46, 1974 p 3.

10) Gieroszynski, A., Sujak, B., ACTA PHYSICA POLONICA, Vol 28, 1965 p 311.

11) Nakayama, K., PROCEEDINGS FROM THE 68TH GENERAL MEETING, JAPAN MACHINERY SOCIETY, Vol C, Tokyo, 1991.

Tribological Characteristics of Oil-Lubricated Ceramics

926C0070B Tokyo DAI 12-KAI SENTAN GIJUTSU FORAMU in Japanese 14 Feb 92 pp 6-11

[Article by N. Imazumi, Business Research Institute, Idemitsu Kosan Co.]

[Text]

1. Introduction

Ceramics with such excellent advantages as heat resistance, hardness, light weight and stain resistance have drawn attention as being useful for mechanical parts and sliding members, with a large number of studies currently under way. The applications of ceramics can be roughly divided into the following two, according to purpose: One is the application in which better frictional wear characteristics than those of exisiting metallic materials are expected, and the other is one aimed at using them under ultimate conditions and specific environments which is impossible with existing materials. With the former, lubricating conditions are the same as the existing ones and temperature conditions range from room temperature to about 200°C, thus raising the expections for further bringing out the ceramic characteristics by means of the lubricating oil used.

This article will describe the influence of the base oil composition and additives on the tribological characteristics of ceramics under oil lubrication (frictional wear characteristics).

2. Tribological Characteristics of Ceramics under Lubrication

2.1 Tribological Characteristics During Nonlubrication

A discussion of tribological characteristics during lubrication requires knowledge of tribological characteristics during nonlubrication. Figures 1 and 2 [not reproduced] show the relationship between μ and the sliding velocity of silicon nitride under a dry air atmosphere and an air atmosphere with relative humidity of 40 percent, respectively. In the dry air atmosphere, μ exhibits values as high as 0.8 to 0.85. On the other hand, humidity has a great influence, confirming that the presence of water greatly reduces μ. Figure 3 [not reproduced] shows the temperature characteristics of μ under an air atmosphere with relative humidity of 40 percent. At 200 to 600°C, relatively low μ values of 0.2 to 0.3 result. Figure 4 [not reproduced] shows the change in μ with PV values for combinations of dissimilar materials. Combinations of ceramics and metallic composite materials (SL alloys), including solid lubricating materials, could noticeably control friction and wear under any conditions. However, μ is high for other combinations. From these results, it follows that the application of ceramics when making mechanical parts is difficult under nonlubrication, and that lubricating oil is necessary.

2.2 Tribological Characteristics under Oil Lubrication

Figure 5 compares the μ values for various ceramics under oil lubrication. It is found that while decreases in friction depend on the lubricating oil, friction characteristics differ greatly according to the type of ceramic. Figure 6 shows μ values of various silicon nitrides, differing in manufacturing conditions and assistants, under polyphenylether. It is found that μ values are lower for combinations of dissimilar materials than for those of similar ones. Figure 7 shows the results of an examination of the influence of combined materials on silicon nitride wear. While the specific abrasive loss of silicon nitride differed depending on the combined steel materials, the specific abrasive loss of steel materials was virtually equivalent.

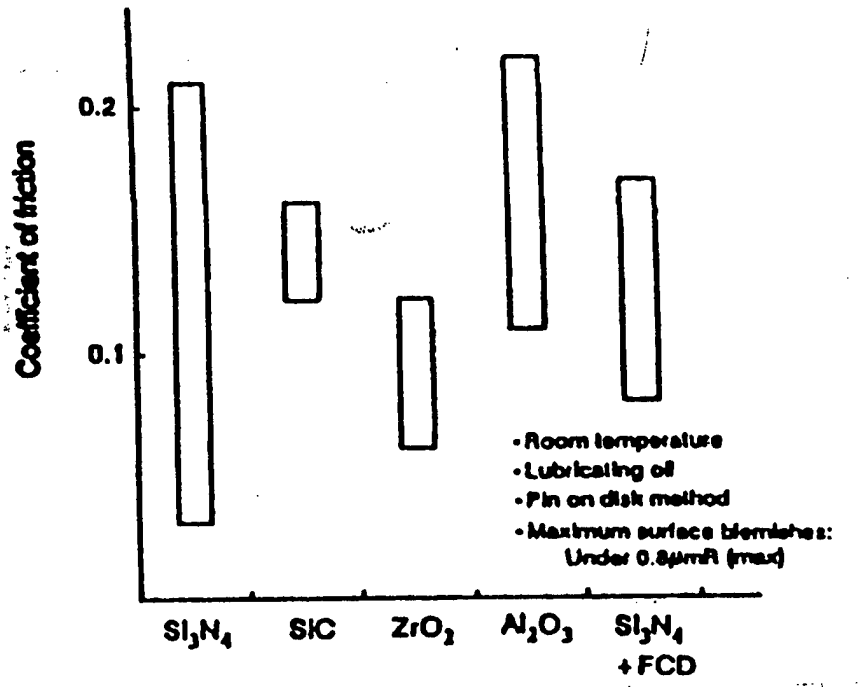

Figure 5. Friction Coefficients of Various Ceramics

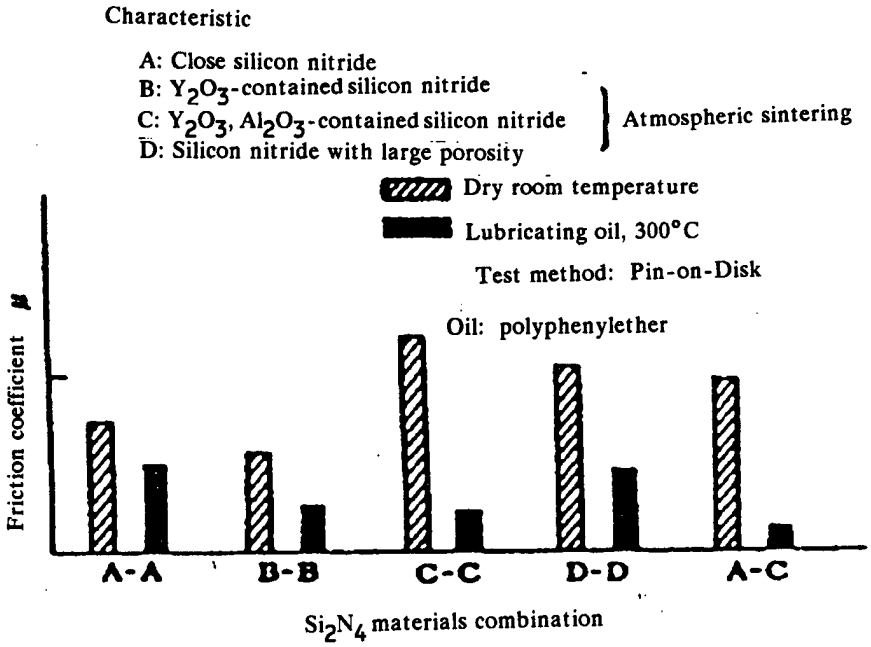

Figure 6. Friction Coefficient of Si_3N_4

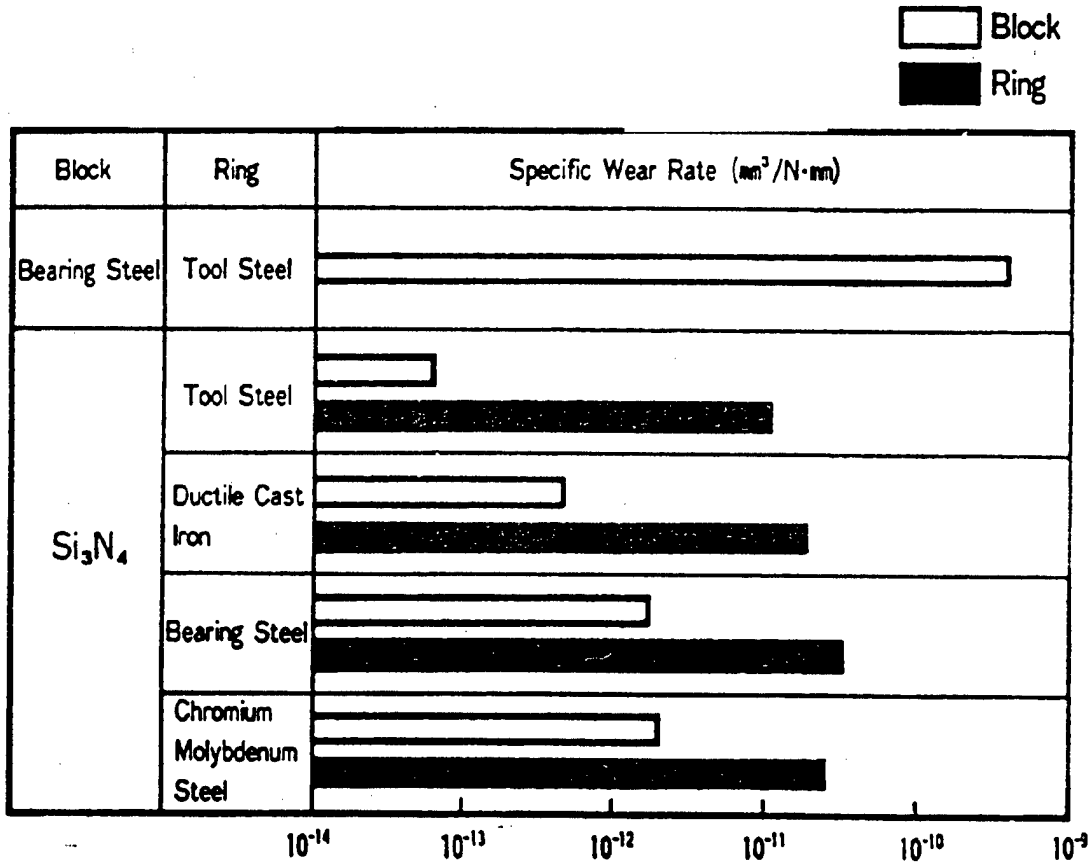

Figure 7. Specific Wear Ratios of Silicon Nitride and Various Steel Materials in Combinations

3. Influence of Base Oil Composition and Additives on Ceramic Oil Lubrication

3.1 Influence of Base Oil Composition

Table 2 shows the friction characteristics of various combined ceramics and ceramics combined with steel using various base oils. These results show that silicon base oil, exhibiting different behavior from other base oils, provides high μ values for any combination. Figure 8 [not reproduced] shows the results of an examination of the influence of PFPE on frictional wear under a dry nitrogen gas atmosphere. For the PFPE/SiC combination, μ values are unstable, with the same base oil exhibiting different behavior for different materials.

Table 2. Friction Coefficients When Combining Various Materials

Pin/Disk	$Si_3N_4^{(*)}$/ $Si_3N_4^{(*)}$	$M50^{(+)}$/ $Si_3N_4^{(*)}$	SiC/SiC	M50/SiC	WC/WC	M50/WC	M50/M50
Lubricant							
None	0.17	0.15	0.52	0.29	0.34	0.19	0.54
Hydrocarbon base oil	0.13	0.11	0.14	0.13	0.18	0.13	0.12
Ester base oil (MIL-L- 23699)	0.12	0.11	0.18	0.13	0.18	0.14	0.13
Silicon base oil	0.24	0.36	0.23	0.42	0.40	0.39	0.35

(*): Grinding finish, 0.64 μm AA (+): M50: Tool steel, hardening, annealing (approx. Rc 60)

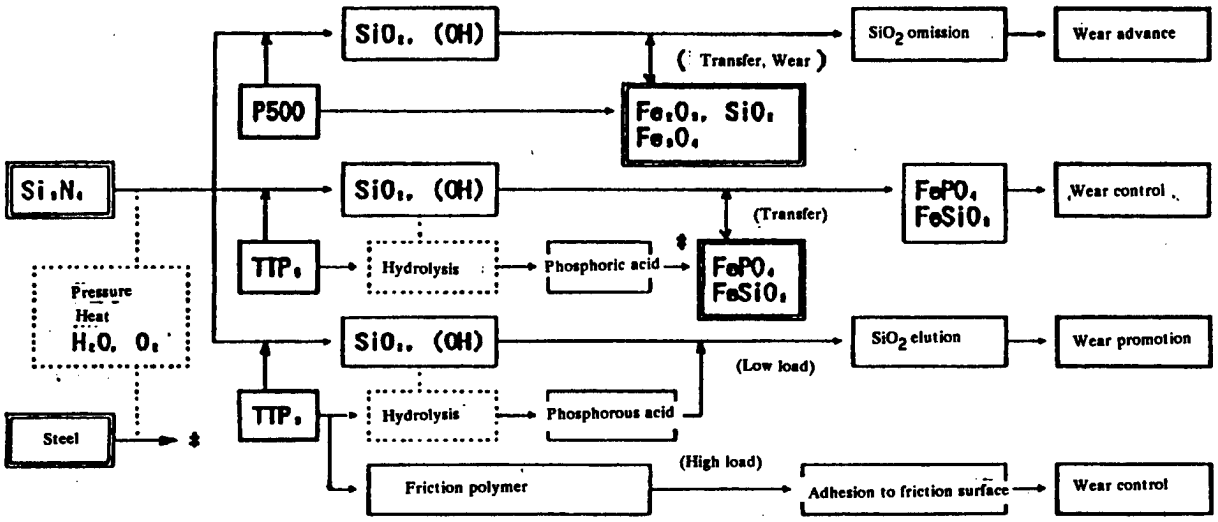

Figure 17. Wearing Process of Si_3N_4 Block in Steel Ring/Si_3N_4 Block Lubrication

3.2 Influence of Additives

Figure 9 [not reproduced] shows the results of an examination of the influence of various additives on the wear of zirconia (FS, PSZ), zirconia in a silicon nitride-steel combination and silicon nitride blocks. TCP and SP extreme pressure additives to silicon nitride reduce wear remarkably, suggesting that good lubrication can be expected under high load conditions. Figures 10 and 11 [not reproduced] show the results of examinations of the influence of different types on wear with respect to phosphorus additives, whose wear preventive effect on silicon nitride has been approved. These results show that phosphate and alkylphosphite groups show wear prevention, but that allylphosphite does not. Figures 12, 13, 14 and 15 [not reproduced] show block friction/wear characteristics under high load (1780N) for various combinations of specimens. These results suggest that when silicon nitride is used for a ring (rotary specimen), low wear lubrication is possible, irrespective of the oil seeds, that wear is great when the mating block (fixed specimen) is steel, and that when steel is used for a ring, good friction/wear characteristics can be obtained by the proper lubricating oil.

4. TCP's Wear Preventive Mechanism

With respect to the wear characteristics in the silicon nitride/steel combination in Figure 13, a surface analysis was made of the friction surfaces when a mineral base oil and TCP blended oil were used, with the products confirmed in Figure 16 [not reproduced]. From the results, the wear process of the silicon nitride block in the silicon nitride/steel combination is thought to be as shown in Figure 17.

5. Conclusion

The same ceramics provide different tribological characteristics depending upon their manufacturing processes, assistants, combined materials and oils. To utilize the excellent characteristics of ceramics, it is desired that more suitable lubricating oils be developed.

Tribological Characteristics of Specially Lubricated Ceramics

926C0070C Tokyo DAI 12-KAI SENTAN GIJUTSU FORAMU in Japanese 14 Feb 92 pp 12-17

[Article by N. Sasaki, Mechanical Engineering Laboratory]

[Text]

1. Introduction

With ceramics viewed as sliding members, it can be said that their first characteristic lies in their hardness. When wear resistance is required for materials, the first thought may be of hardness. It is unreasonable to jump to the conclusion that there is a relationship between hardness and wear resistance without discussing wear forms. When a problem involving wear in general arises, however, it is abrasive wear that is involved in most cases. Since hardness is an important parameter for controlling

abrasion loss through abrasive wear, much is expected from ceramics as a wear-resistant material.

The second characteristic lies in the bonding form of atoms. In a friction interface, deformation and coagulation occur with relative ease in intermetallic bonding where no intense bonding directionality exists, making it difficult to keep the surface in the initial state. On the other hand, since ceramics consist of covalent and ionic bonds, deformation and coagulation occur with difficulty unless they are in the final wear state where brittleness is dominant, making the surface state is easy to retain.

What characteristics do ceramics have when viewed in terms of lubrication? When lubrication mechanisms are divided into fluid lubrication and boundary lubrication, the lubrication characteristics are determined by surface roughness in the former and by the compatibility between the surface and a lubricant in the latter. Regarding surface roughness for ordinary lubrication, ceramics excel in processibility, precision and stability, and can be said to be materials suitable for fluid lubrication. On the other hand, although generalization should be avoided since various complicated factors relate to their compatibility with a lubricant, when assessing their chemical activities (adsorption activity, catalytic activity, etc.), an important index, it can be said that they are remarkably inferior to metals. Since ceramics enable a friction surface to be retained easily, as stated above, and, consequently, integrated results of surface reactions are reflected in tribology, the atmospheric effect ignored heretofore sometimes results in remarkable lubrication. As shown in Table 1, the atmospheric effect of ceramics on tribology can probably be divided into three stages. Based on the tribological characteristics of ceramics in various atmospheres, this article will describe the feasibility of specific lubrication utilizing an atmospheric effect mechanism and these characteristics.

Table 1. Mechanism of Atmospheric Effect on Friction and Wear of Ceramics

1. Formation of adsorption layer
2. Change in mechanical properties of friction surface following adsorption
2.1. Chemomechanical effect
2.2. Stress corrosion reaction
3. Tribochemical reaction

2. Underwater Friction/Wear Characteristics

Figures 1 to 4 [not reproduced] show the friction/wear characteristics of various ceramics in water and a water solution. With silicon nitride and silicon carbide, the friction coefficient shows an extremely low value of about 0.01 in a high friction velocity area. This seems to result from the state of fluid lubrication formed by the slight elution of a hydrate due to tribochemical reaction in a friction surface and the consequent flattening of the friction surface. The increased viscosity of the water solution by adding a water soluble polymer or glycol is effective for improving the friction and wear characteristics in a low velocity area (Figure 2). Alumina excels in wear characteristics, showing a relatively high friction coefficient of 0.3, with no velocity dependence observed. This seems to result from little elution of alumina to water, and its increased elution by varying the pH enables the friction coefficient to be reduced (Figure 3). Fatty acid salt, as an additive, acts effectively to improve the friction characteristics of alumina (Figure 4). With zirconia, the water-caused stress corrosion transformation reaction is further promoted by friction, resulting in severe wear.

3. Friction/Wear Characteristics in Organic Compounds

Figure 5 [not reproduced] shows the friction/wear characteristics of silicon nitride in an organic compound vapor atmosphere. Although the lubrication effect by vapor compounds can be observed in any atmosphere, in acetone, hexane and benzene atmospheres, in particular, friction polymers were observed to be produced in a friction surface, thus obtaining good lubrication characteristics. Figure 6 shows the friction characteristics of alumina in organic solutions. The load dependence of the lubrication effect differs according to the solution. The lubrication mechanism of organic solutions can be understood as follows by comparing it with the adsorption activity shown in Table 2. In a low load area, friction reduction by adsorption films becomes dominant, while in a high load area, lubrication by tribochemical reactants becomes dominant. For example, diethyl ether, which is superior in adsorption characteristics but inferior in adsorption film strength, cannot be expected to provide lubrication in a low load area. Also, for a solution remarkably inferior in adsorptivity, such as hexane, lubrication by tribochemical reaction reactants can be expected in a high load area.

Table 2. Adsorption Activity in Alumina Friction Surface

Order	Adsorption Activity	
	Adsorption Velocity	Adsorption Strength
1	Acetone	Diethyl ether
2	Diethyl ether	Methyl alcohol
3	Methyl alcohol	Acetone
4	Water	Water
5	Benzene	Benzene
6	Hexane	(Hexane)

4. Friction/Wear Characteristics in Vacuum

Figure 7 shows the friction characteristics of various ceramics in a nitrogen low pressure atmosphere. Tending to begin to decrease around 10^{-2} Pa, exhibiting a minimum value in a low vacuum area, and then increasing again, no pressure dependence of the friction coefficient can be observed in a high vacuum area of below 10^{-3} Pa. The pressure at which the friction coefficient begins to decrease virtually agrees with 2×10^{-3} Pa, the pressure necessary for the disk friction surface to

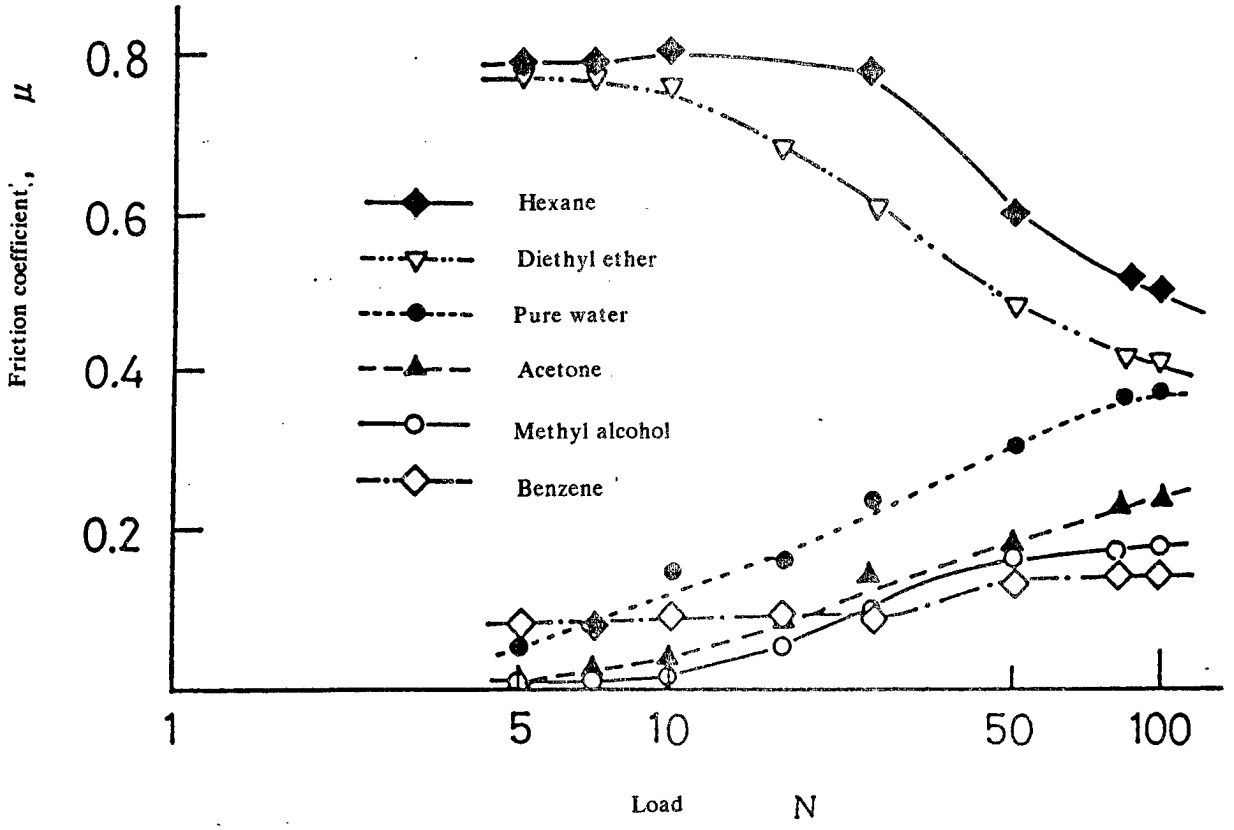

Figure 6. Alumina Friction Characteristics in Organic Solution: Friction Velocity, 0.2 m/s

obtain incident molecules corresponding to 1 Langmuir and form a monomolecular adsorption layer. Figure 8 [not reproduced] shows the wear characteristics of silicon carbide in a nitrogen low pressure atmosphere. The pressure dependence of wear peaks in a low vacuum area. Since this pressure area overlaps with the pressure area where gas discharge is most likely to occur and agrees with the pressure at which change appears in the electrication behavior of a friction surface, as shown in Figure 9 [not reproduced], the discharge and residence behavior of wear-caused powder in a friction surface resulting from static electricity seems to contribute substantially to the manifestation of a peak.

5. Conclusion

The original meaning of lubrication was to relax the shearing resistance through the intervention of a third substance between two solids in relative motion. In ceramic friction surfaces, which are hard to grind and cause deformation and coagulation, the presence of a small quantity of an inclusion enables sufficient lubrication to be obtained. As a result, specific lubrication effectively utilizing the atmosphere becomes possible. Particularly important in specific lubrication is to effectively utilize tribochemical reactions, the detailed mechanism of which is not yet understood very well.

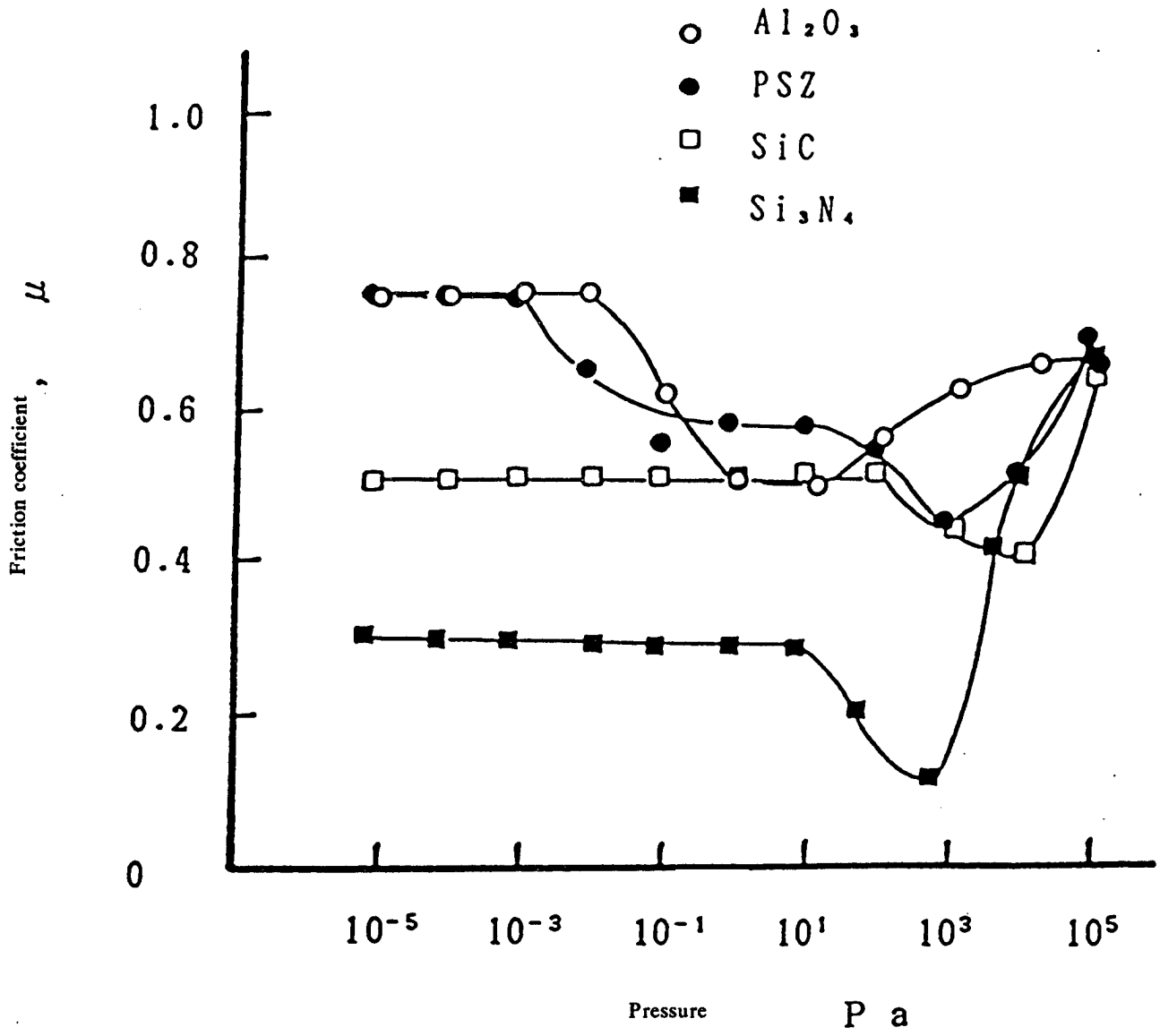

Figure 7. Friction Characteristics of Various Ceramics in Nitrogen Low Pressure Atmosphere: Load, 3N, Friction Velocity, 0.1 m/sec

Tribological Characteristics of High Temperature Lubricated Ceramics

926C0070D Tokyo DAI 12-KAI SENTAN GIJUTSU FORAMU in Japanese 14 Feb 92 pp 18-23

[Article by Y. Enomoto, Mechanical Engineering Laboratory]

[Text]

1. Introduction

Lubrication measures for ceramics in high temperature areas comprise a key technology in the development of equipment driven at high temperatures. This article will summarize research trends to date on the tribology of ceramics at high temperatures.

2. Dry Friction of Ceramics (Oxidizing Atmosphere)

2.1 Combination of Same Group Materials

Reports have been made on the friction/wear characteristics of same group materials under nonlubrication with respect to silicon nitride, silicon carbide, alumina and partially stabilized zirconia (PSZ). However, with a specific abrasion loss Ws exceeding 10^{-7} mm^2/kg, their friction coefficient μ can surpass 0.5. On the other hand, while oxide-group ceramics of TiO_2 and Cr_2O_3 (thermal spray) exhibited high friction (μ = 0.8 to 1.2) at room temperature, unlike the above four types of ceramics, they demonstrated a decrease in [friction] with increasing temperatures, providing 0.45 to 0.6 at 600°C. Also, chromia-sintered ceramics have lower friction coefficients at high temperatures than other ceramics (μ = 0.4).

While silicon-group ceramics, such as SiC and Si_3N_4, and oxide-group ceramics, such as Al_2O_3 and ZrO_2, are inferior in high temperature dry friction, the high temperature friction coefficients of TiC sintered carbides are as low as about 0.2 due to oxide lubrication resulting from high temperature oxidation. As for the friction coefficients of same-group fluorocarbon compound ceramics containing TiB_2, ZrB_2 and B_4C, as shown in Figure 1 [not reproduced], the μ value around room temperature increases rapidly at 0.2, reaching 0.6 to 1.0 around 600°C, then drops rapidly around 700 to 750°C to 0.1 to 0.2. This is because the B_2O_3 generated by the oxidation decomposition of TiB_2 and B_4C melts to form a vitrified fluid layer in the friction surface, resulting in lubrication.

2.2 Combining Ceramics with Metals

When ceramics are rubbed with metals (M-50 and Inconel 718), which excel in high temperature strength characteristics, both the friction coefficient and wear decrease at high temperatures compared to their values at room temperature. In such cases, these values are lower than the case of same- group ceramics. Figure 2 [not reproduced] shows experimental results obtained by a NASA group by comparing the friction coefficients and wear at room temperature and 800°C. Any combination provides a friction coefficient of about 0.3 at a high temperature of 800°C, while wear is greatly affected by material combinations. A combination of mullite or silicon nitride with Inconel results in the least wear. At high temperatures, a metal is oxidized to cause delamination in the interior of the oxide film, thereby promoting oxidation wear. However, the lubricating action of this oxide results in low friction.

3. Dry Friction of Ceramics (Nonoxidizing Atmosphere)

According to the results of Yust, et al.'s investigation of the friction and wear of combinations of same-group materials, including SiC, Si_3N_4, PSZ and Al_2O_3, and dissimilar materials in a range between room temperature and 400°C in nitrogen, every combination exhibited values as high as 0.7 to 1.0 at any temperature, except for a PSZ friction coefficient of 0.24 that was recorded. A combination of SiC, Si_3N_4 and PSZ provided the least wear. Figure 3 shows the high temperature wear characteristics of silicon nitride. The friction coefficients of carbides (SC, NbC, TaC and B_4C) and boride (TiB_2, ZrB_2) in a low vacuum, as shown in Figure 4 [not reproduced], decrease with increasing temperatures in a range higher than 1,000°C, rapidly increasing later. It is regarded that, in a temperature range lower than around 1,000°C, a true contact area undergoes virtually no change, the coagulation between crystals decreases, and these ceramics consequently become easy to shear, with friction decreasing with the temperature.

On the other hand, it has been confirmed that, at temperatures exceeding 1,400°C, intergranular diffusion occurs, coagulation increases and the material itself softens, thus resulting in an increase in the true contact area and high friction. As shown by the broken lines in Figure 4, a combination with graphite enables the friction in high temperature areas to be reduced.

Rubbing α-SiC with iron in a vacuum causes adsorbed matter to be removed at around 300°C, with the friction coefficient rapidly increasing from 0.4 to about 1.0. However, because of the frictional heat decomposition of SiC into Si and graphite, the friction coefficient resumes a low friction value of about 0.4 from around 300°c.

4. Lubrication (Lube) of Ceramics

The temperature range to which oil is applicable is that approaching 300°C. Figure 5 [not reproduced] shows the temperature and life limits of synthetic lubes. Lubes withstandable to high temperatures of up to 260°C include polyphenyl ether, neopenthilpolyol ester, C-ether (thioether), polyfluoropolyalkyl ether (PFAE), silahydrocarbon and polyolester deuteride (PEdTH). A new attempt in a higher [temperature] area by Lauer, et al., involves the continuous production of carbon films on ceramic surfaces by ethylene contact reduction and, consequently, the achieving of low friction.

The author, et al., examined the applicability of various coatings, including ceramics, on the friction surface, using 50 ml of polyphenyl ether which reportedly excels in heat and radiation resistance. An SRV microreciprocating friction tester was used for testing the friction and wear between the coating disk and a ball bearing 10 mm in diameter at room temperature and 250°C. Figures 6 and 7 show the initial and steady-state values of the friction and wear depths of the balls and disks at room temperature and 250°C. As shown by this diagram, a Cr_2O_3 sintered film, salt bath nitriding and oxygen nitriding demonstrated relatively good results.

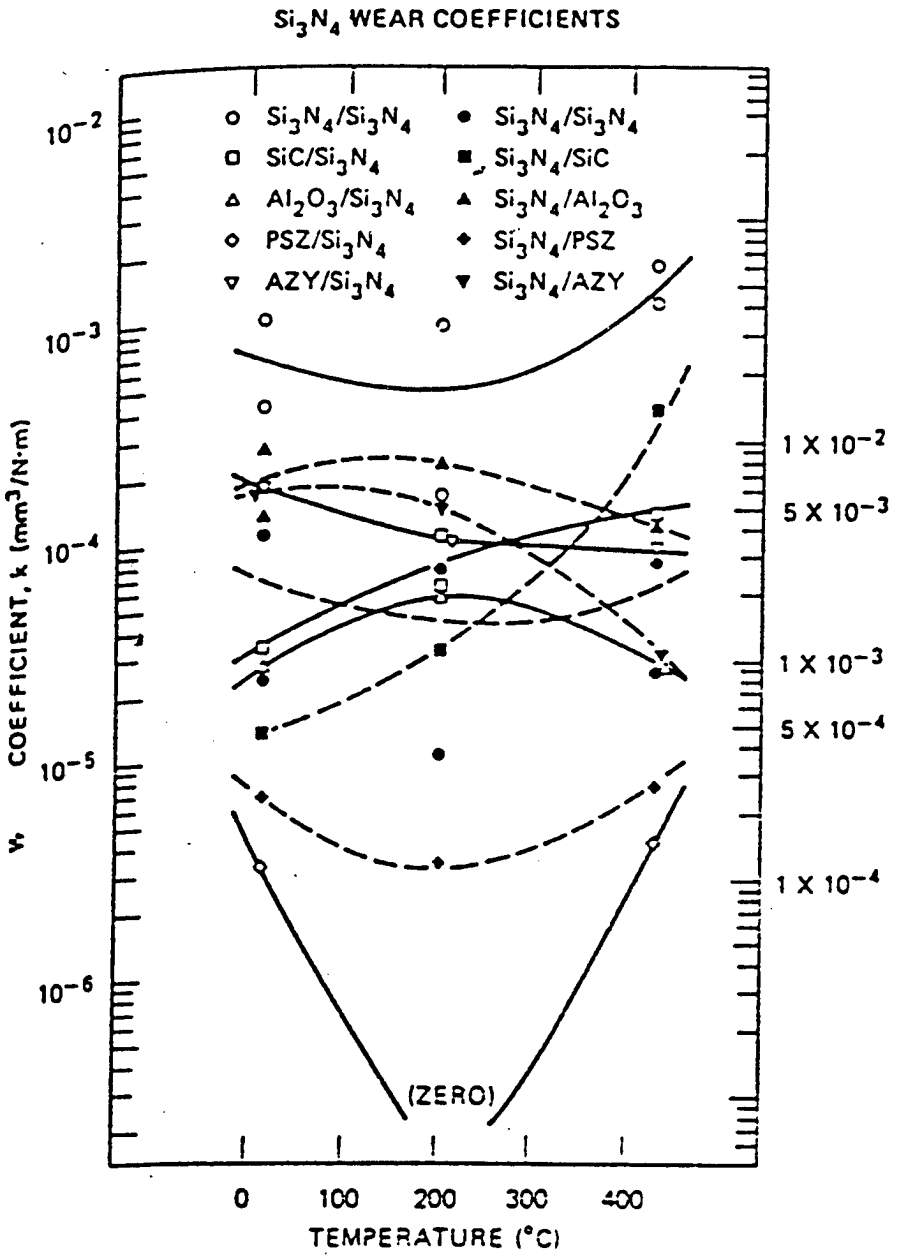

Figure 3. Wear Temperature Characteristics of Silicon Nitride: Pin disk; Load, 9 N; Velocity, 0.3 m/sec

Figure 6. Microsliding Friction and Wear of Coating Agents Under Polyphenyl Ether Lubrication (Room Temperature)

Surface Treatment/Coating	Average Friction Coefficient		Abrasion Loss	
	Initial Value	Final Value	Ball (mm)	Disk (m)
	* major fluctuation			
Cr_2O_3 sintered film	0.17	0.19	0.68	<1-2
Cr_2O_3 injected film	>0.4 *	0.34	2.3	<1
TiO_2 injected film	>0.35	0.21	1.2	3-4
Triballoy injected film	0.25	0.15	1.14	4
CrN ion plating	0.16*	0.21	1.05	4.8
Cr_2N ion plating	0.35*	0.15	1.3	2
Salt bath soft nitriding	0.18	0.145	0.68	4-5
Oxidation soft nitriding	0.17*	0.14	0.8	5
Boriding	0.37*	0.19	1.14	3
Carburization chromizing	>0.4 *	0.35	2.8	<1.2
PTFE spray coating	0.17-0.25	0.18	1.27	3.8
Nitrogen ion injection	0.35*	0.12	0.885	6
Untreated bearing steel	>0.4 *	0.19	1.25	4-5

5. Solid Lubrication of Ceramics

The dry friction characteristics of ceramics at room temperature and in high temperature areas sometimes result in low friction due to the oxidation reactions caused under limited conditions, but no stable friction characteristics can be obtained at from room temperature to high temperatures. The application of ceramics as a tribomaterial in a high temperature area exceeding the service limitations of oil cannot help but rely on solid lubricants. The following process represents a major theme to be solved in the future.

5.1 Solid Lubrication in Vacuum

Figure 8 [not reproduced] shows the results of rubbing Si_3N_4 containing ground MoS_2 in the atmosphere and a vacuum. While the solid lubrication effect can be observed up to around 500°C in the atmosphere, during the temperature reduction process, there is no evidence that the lubricant has oxidized and deteriorated. In a vacuum (10^{-5} Torr), on the other hand, the lubrication effect can be observed, to some extent, up to around 900°C.

5.2 Solid Lubrication in Oxidizing Atmosphere

As shown in Figure 9 [not reproduced], general purpose solid lubricants, such as MoS_2 and WS_2, are effective up to about 500°C, while the application of other materials for solid lubrication is desired at higher temperatures. Under such circumstances, the lubrication of TiNi and Co ion-evaporated films, vacuum evaporated films, and CaF_2/BaF_2 impregnated foaming Ni is being tested. Ion injection into TiNi and Co films reduces the friction coefficient to from 0.06 to 0.09 at 800°C. In this case, Ni, Ti and Co oxide films have resulted in lubricating action.

Being stable at high temperatures in the atmosphere, oxides are raising great expectations for the high temperature lubrication of ceramics. Table 1 [not reproduced] lists the high temperature friction characteristics of oxide solid lubricants examined to date as summarized by Allam. Oxide solid lubricants which show stable friction coefficients at from room temperature to high temperatures (< 800 to 1,000°C) are not currently available. It is apparently necessary to examine the lubricity of polyphyletic (e.g., binary or ternary) lamellar oxides and develop materials in the future. High temperature superconductive materials happen to have such a crystal structure, and the progress in materials science in this field will be worth watching. In fact, an experiment by the author and his group has found that, as shown in Figure 10, the friction of the Y-Ba-Cu-O group did not become as low, but instead was stable up to high temperatures. Nastasi, et al., however, claim that the friction of the evaporated films of Y-group superconductive oxides at room temperature is high.

The author and his group have recently tackled the problem of finding good candidates from among the polyphyletic oxides used as dielectric materials, confirming that a Na_2ZrO_3 and $Cr_2)O_3$ double oxide coating demonstrates interesting low friction behavior with alumina friction. Figure 11 shows its results. The likelihood of promoting the development of such oxide solid materials is likely to provide momentum for the development of full-fledged self-lubricating ceramic composite materials.

6. Conclusion

While the current status of the high temperature tribology of ceramics has been described, this field still has a long way to go. The development of new materials (solid lubricants, lubes, etc.) and new lubricating methods is desired. To this end, tribology specialists should present new material design guidelines based on the characteristics they have evaluated, and feed it back for use in the development of new tribology materials.

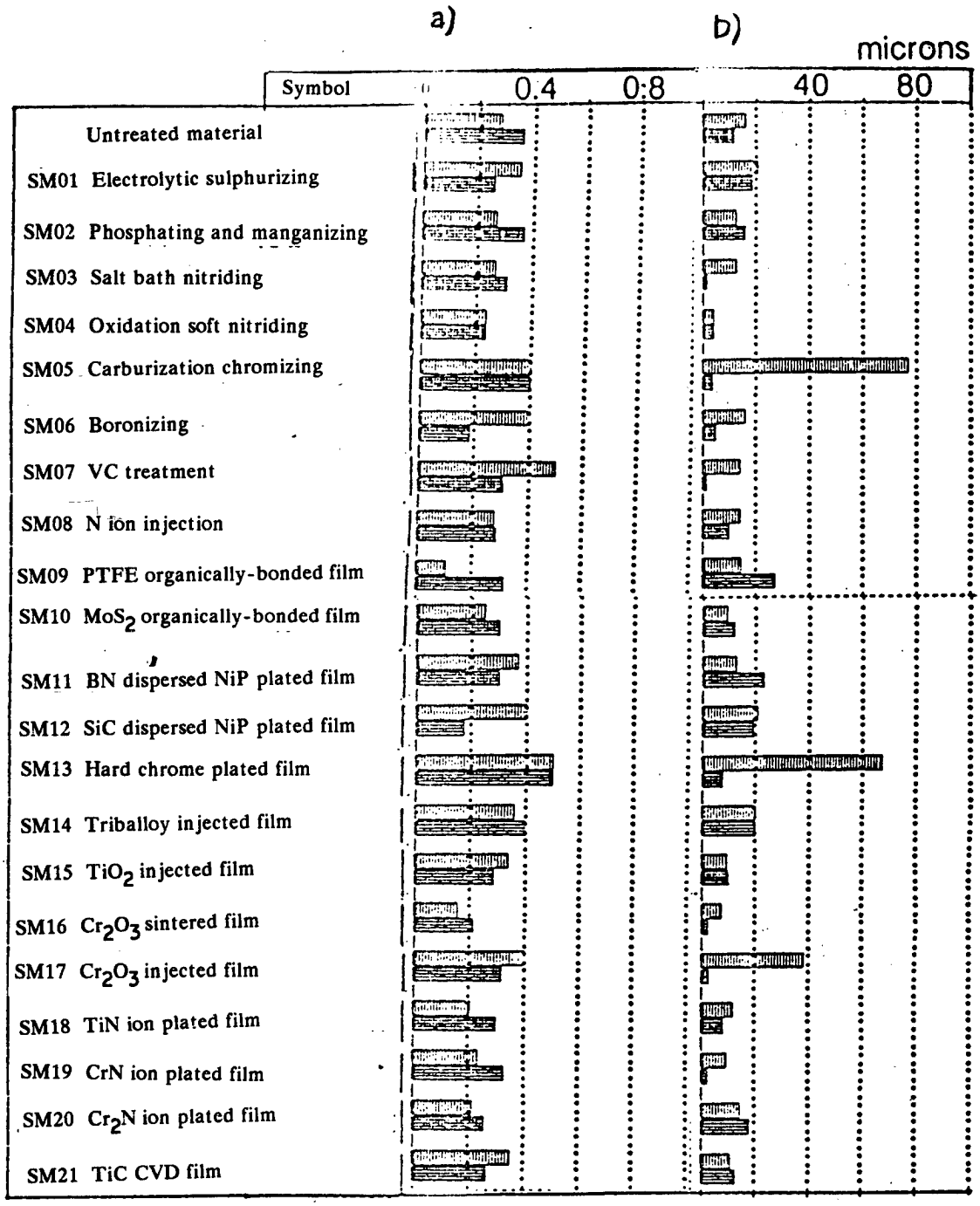

a) Friction coefficient (top: initial value; bottom: steady-state value)

b) Wear depth (top: ball; bottom: coating disk)

Figure 7. Microsliding Friction and Wear of Coating Agents Under Polyphenylether Lubrication (250°C)

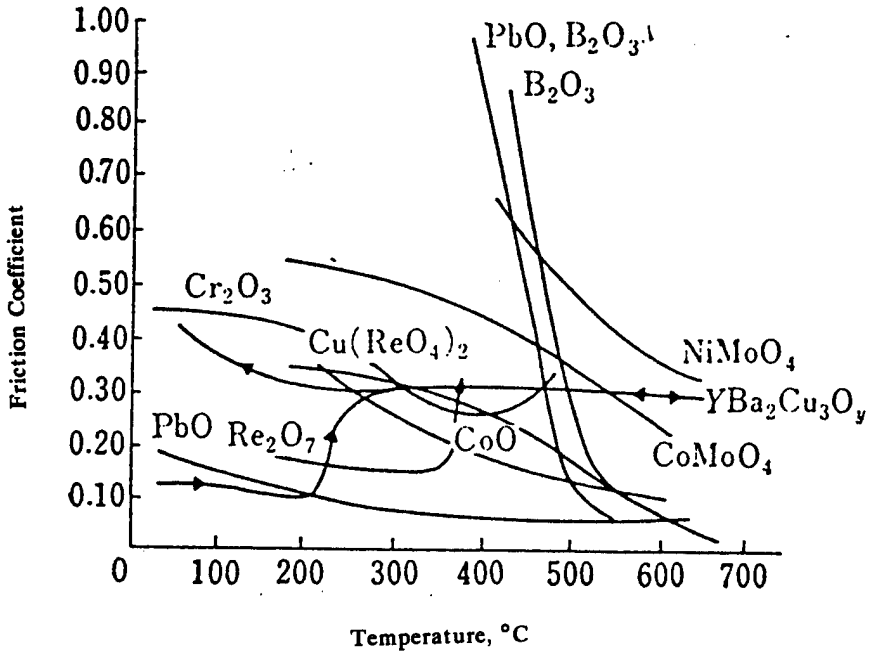

Figure 10. High Temperature Friction Characteristics of Y-Group Superconductive Oxides and Other Oxides

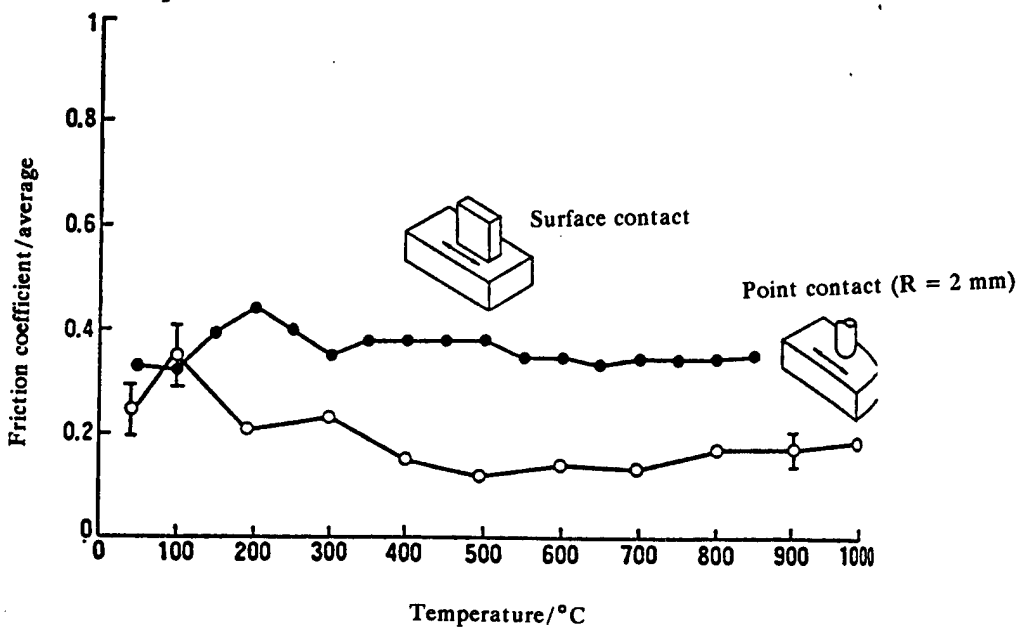

Figure 11. High Temperature Friction Characteristics of Double Oxide Coating of Na_2ZrO_3 and Cr_2O_3

Frictional Control by Impresed Voltage

926C0070E Tokyo DAI 12-KAI SENTAN GIJUTSU FORAMU in Japanese 14 Feb 92 pp 24-28

[Article by Y. Yamamoto, Institute of Science Technology, Kanto-Gakuin University]

[Text]

1. Introduction

Dissimilar metals rubbing each other not only generate heat, but also cause electric phenomena to occur. Assessing this, the author has contrived a method for artificially controlling the induced voltage generated by the friction between dissimilar metals, finding that this method enables friction coefficients, wear ratios and wear energy to be adjusted. Since conventional research on tribology did not take such electric phenomena, and induced voltage in particular, into consideration, this study has demonstrated it for the first time.

2. Generation of AC and DC Voltages by Solid Friction

The strength of the electric field induced on the friction surface was measured through a dry wear test of an ordinary cast iron (FC20) rod relatively combined with a mechanical structural steel ring (S35C) under wear test conditions of a surface pressure of 10.2 kgf/cm^2 and a friction velocity of 118 m/min, under a room temperature atmosphere, with a maximum induced voltage of 1.0 mV. In this experiment, the rod and ring were connected to the negative and positive electrodes, respectively. It has been reported that steel normally enables an oxide film of 1,000 Angstroms to be produced in the atmosphere. Assuming that an oxide film of 1,000 Angstroms exists between the two electrodes (rod and ring), a very large value of their electric field strength can be obtained as follows:

$(1.0 \times 10^{-3}\ \text{V})/10^{3} \times 10^{-8}\ \text{cm} = 10^{2}\ \text{V/cm} = 10^{4}\ \text{V/m}$

Therefore, the electric energy effect by this large electric field cannot be neglected with actual friction surfaces.

A study of induced voltage by friction and wear includes one on the surface temperature of the wearing surface measured as a thermocouple by Bowden, et al., as shown in Figure 1 [not reproduced], i.e., one applying the thermoelectric potential difference induced between relative wearing specimens. The study has revealed that a high temperature occurs and ceases to exist on the wearing surface in the short time of 10^{-4} seconds, that this corresponds to the time required for the rupture of the true contact point to occur, and that the flash temperature, i.e., the temperature corresponding to the maximum point of the thermoelectric potential, becomes high at the true contact point.

The author and his group conducted a sliding dry friction test combining same-group constantan and a copper thermocouple material (Figures 2 and 3 [not reproduced]). Due to mechanical cumulative work and the friction distance, the work was divided into an initial and steady regions in proportion to the friction distances, and branch points where straight lines taking different inclinations could be observed. From the relationship between the induced voltage (ac and dc) and the friction distance, the ac electric potential difference was generated in the steady region, which relates to tribology. Furthermore, looking at the relationship between the friction coefficients and friction distance, the occurrence of induced voltage drops in accordance with the static friction coefficient, with the dynamic friction coefficient again exceeding the static friction coefficient and a large dynamic friction coefficient beginning to appear in the constant region.

General materials are smaller in dc potential difference and greater in ac potential difference than are thermocouple materials. The availability of dc and ac potential differences was confirmed in the steady region where wear progresses. The ac voltage handled in this article refers to nonperiodic, strain-waveform voltage, just as is shown in frequency analysis, rather than general periodic alternating voltage.

Figures 4 and 5 [not reproduced] illustrate the frequency analysis of the induced voltage generated during sliding dry friction and the wear between a WC sprayed film and SUJ2 bearing steel, and the relationship between dc and ac voltages and the friction distance, respectively.

This research has developed a measuring system combining a device for artificially controlling the induced voltage generated by the wear between relative metals with peripheral equipment, enabling the friction coefficients, wear ratios and wear energy to be adjusted (Figure 6 [not reproduced]).

3. Frictional Control by Impressed Voltage

An adjustment device for the induced voltage (ac and dc) generated by sliding dry friction was developed, and the antifriction effect by an induced voltage (ac and dc) adjustment method for artificially controlling the induced voltage generated by friction and wear when a carbonized tungsten (WC) plasma-sprayed film and bearing steel are placed in a high temperature oxidizing atmosphere was examined (Table 1). The experiment has confirmed, with the use of the induced voltage adjustment method proposed by the author, that wear conditions causing wear ratios to change quantitatively exist, confirming the antifriction effect.

Table 1. Antifriction Effect by Induced Voltage Adjustment Method

Relative Material (1st item, Rod; 2nd item, Ring)	Frictional Conditions (surface pressure kgf/cm^2; friction velocity m/min)	Decrease in Friction Coefficient (1st value, 450°C; 2nd value, 20°C)	Decrease in Wear Ratio (1st value, 450°C; 2nd value, 20°C)
SUJ2; Wc-12Co self-melting alloy-sprayed film	3.4; 50	0.75 → 0.7 (6.6%); 0.65 → 0.6 (7.6%)	45%; 25%
SUJ2; Wc-17Co sprayed film	3.4; 25	0.87 → 0.72 (18%); 0.68 → 0.25 (64%)	20%; 70%)
SUJ2; Wc-17Co sprayed film	3.4; 50	0.78 → 0.70 (11%); 0.65 → 0.60 (8%)	46%; 25%
SUJ2; Cr_2O_3 sprayed film	3.4; 50	57.4%); 0.8 → 0.64 (20%)	15%; 79%
SUJ2; S45C	3.4; 50	0.66 → 0.64 (3%); 0.66 → 0.62 (5%)	41%; 12%
Constantan; Copper	2.98; 10	—; 0.837 → 0.267 (68%)	—; 60%
SUJ2; Cr_3C_2 sprayed film	3.4; 50	0.81 → 0.76 (6%);—	82%;—

In order to obtain microinformation on a friction surface, a detailed analysis by an X-ray microanalyzer (EPMA) of the friction surface tested in the atmosphere was made, thereby verifying the presence of metallic oxides, such as FeO, Fe_2O_3, WO_2, WO_3 and NiO. These are all known as oxide semiconductors, raising expectations for the manifestation of electronic phenomena unique to semiconductors on friction surfaces. In other words, a friction surface can conceivably be a contact interface between a metal and an oxide semiconductor. In general, in a junction interface between a metal and an n-type semiconductor, electrons flow from the semiconductor side to the metal side when the work function of the metal is greater than that of the semiconductor, forming a space charge layer in the neighborhood of the interface, and resulting in so-called rectification characteristics. Therefore, properly adding a dc current from the exterior enables an electron current to be controlled. This phenomenon is the intrinsic principle of controlling electric energy in this research. Likewise, a current can be controlled by external voltage in metallic p-type semiconductors as well. In reality, ohmic contact sometimes results, depending on the type of substance comprising the contact interface. In any case, a technical approach for controlling a current by external voltage has been established. Such electric phenomena have not been considered at all in conventional research on tribology.

Direct linear and surface analyses of a wearing surface were conducted using EPMA, confirming the oxide films produced on metal surfaces in relative motion and their turning into semiconductor films (Figures 7 and 8 [not reproduced]).

The induced voltage was measured in succession and confirmed the ease/difficulty of the current flow in materials with a pronounced polarity change, thereby demonstrating the existence of such a phenomenon resulting from the oxide semiconductor characteristics. In other words, a study has been made of a method for dividing the total energy required for wear into mechanical and electric energy, without neglecting the latter, changing it by impressing the external voltage, and thereby reducing the friction ratio and friction coefficient (Figure 9 [not reproduced]). Since electric energy is as small as less than 10^{-18} of mechanical energy, with the exception of specific points, a strong correlation was observed between the two. As for the induced voltage, an ac potential difference was found in the steady region and a dc potential difference in the total area, including the transition regions, proving that they will be factors involved in wear.

4. Effect and Potential

This research has demonstrated by wear tests in the atmosphere and at high temperatures that friction coefficients and abrasion loss can be reduced by impressing the external voltage inversely to the voltage induced during sliding dry wear. The research also points out that oxide semiconductors are produced on a wearing surface, that their electric characteristics differ according to the junction sequence of the metals and semiconductor films, and that a greater effect can be obtained at high temperatures than in the atmosphere by taking the induced voltage into consideration. Sliding dry wear testing by surface contact was conducted, and it is apparently possible for the induced voltage adjustment method to be applied under linear contact conditions. It is conceivable that this method can be applied to point or surface contact, such as "rolling wear," when it is dry. Moreover, in wearing phemonema on surfaces of clean materials in a supervacuum, the friction coefficients increase unexpectedly and, at the same time, the abrasion loss becomes zero. The author's induced voltage adjustment method is also likely to be applied to such cases. Thus, friction and wearing phenomena in a vacuum represent a basic problem when studying wearing mechanisms, and the method is likely to be applicable to members sliding in a vacuum.

In addition to the above, it is expected that the induced voltage adjustment method will be applicable when developing supercompact bearings for mechatronics parts and adjusting the friction coefficients of equipment with components and parts involving frictional sliding, such as clutches, gears, brakes, and rollers. In particular, its application to equipment with power transmission devices, such as vehicles, will be extremely useful, and is expected not only to reduce the abrasion loss of the sliding units of machines, but also to greatly contribute to reducing the mechanical friction energy loss and to

Application of This Research and Its Applied Fields in the Future

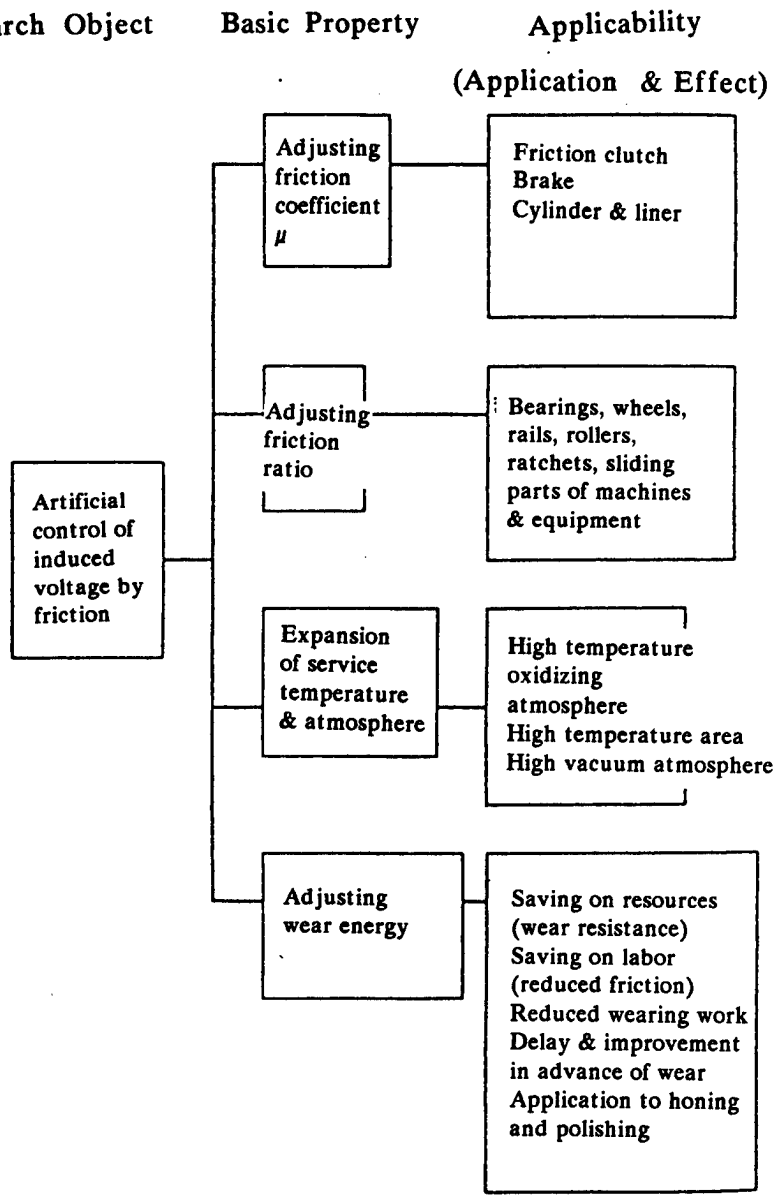

increasing the total energy efficiency. This article has discussed the influence of friction and wear when the friction coefficients are adjusted so as to offset the induced voltage. Moreover, intentionally applying impressed voltage to a wearing surface is likely to lead to the application of this method to honing and polishing. For example, it is likely to substantially shorten the time required to break in pistons and cylinders of internal combustion engines, as well as bearings. Furthermore, it can be applied to machining. Thus, the knowledge gained through this research is likely to be widely applied industrially.

5. Conclusion

This research has shown that abrasion loss and friction coefficients can be reduced by externally applying

impressed voltage to induced voltage (ac and dc) between various metals in relative frictional motion and by thus adjusting the friction coefficients so as to offset the induced voltage, and has quantitatively confirmed the antifriction effect through the application of these techniques to commercial metallic materials.

Ceramic Applications to Rolling Bearings

926C0070F Tokyo DAI 12-KAI SENTAN GIJUTSU FORAMU in Japanese 14 Feb 92 pp 40-45

[Article by T. Yoshioka, Mechanical Engineering Laboratory]

[Text]

1. Introduction

With the characteristics shown in Figure 1, ceramics are raising great expectations in terms of expanding the service area of rolling bearings. This article will describe the evaluation of ceramics for use as materials for rolling bearings and general applications of ceramic bearings.

2. Evaluation of Ceramics as Rolling Bearing-Use Materials

2.1 Evaluation In Terms of Rolling Fatigue Strength

Figure 2 [not reproduced] gives examples of experiments conducted by the author's group on the rolling fatigue of ceramics[1),2)]. Figure 2 [not reproduced] shows a test bearing simulating the construction of a thrust ball bearing. The outer ring is a ceramic specimen. Its specifications are: outer diameter of 47 mm and inner diameter of 25 mm for both the inner and outer rings, into which three or six balls, 7.937 mm in diameter, have been incorporated. Figure 3 [not reproduced] shows the testing machine used for the experiment.

Table 1 lists the characteristic values of the ceramics incorporated into the outer ring as a specimen. Figure 4 [not reproduced] presents the experimental results of rolling fatigue as plotted on a Weibull chart. It can be seen from the chart that, with an accumulated damage probability of 50 percent (indicated by the dotted line), hot pressed material A is close to bearing steel in life (L_{50}), while material B, with an accumulated damage probability of 10 percent, exceeds bearing steel L_{10} and L_{50}.

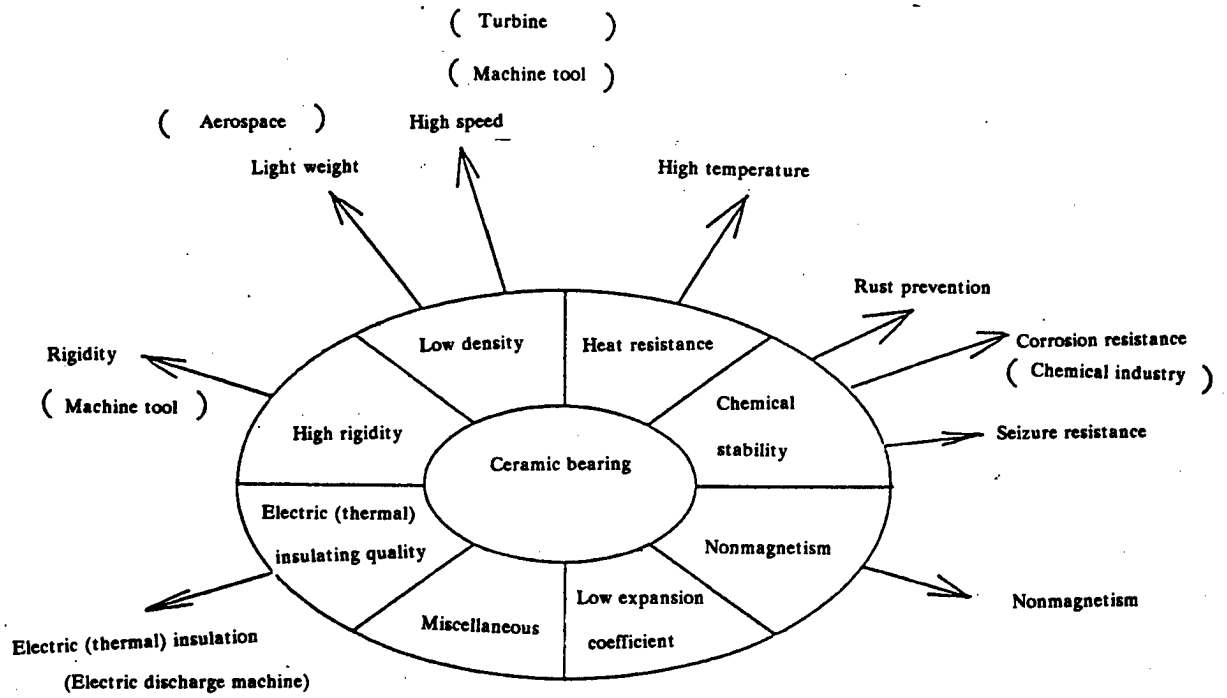

Figure 1. Physical and Chemical Characteristics of Ceramics and Ceramic Bearing Application

Table 1. Characteristic Values of Ceramic Materials

Material	Hardness	Density (g/cm^3)	Bending Strength (MPa)	Young's Modulus (GPa)	Poisson's Ratio
Hot Pressed Materials					
SiC	94.9 (HRA)	3.17	690	402	0.17
ZrO_2	1500 (HV)	6.05	1470	210	0.31
Si_3N_4 A	92.4 (HRA)	3.27	780	304	0.27
B	1800 (HV)	3.21	1040	314	0.26
Bearing steel	62 (HRC)	7.87		205	0.28
	741 (HV)				

Table 2 summarizes the experimental results, proving that hot pressed Si_3N_4 is most appropriate for use as a bearing material. With the weight per ball being about 61 percent that of bearing steel with a maximum contact stress of 94 percent, Si_3N_4 material B is 1.8 and 4.2 times that of bearing steel in L_{10} life and L_{50} life, respectively, while for material A they are 0.438 and 0.492 times, respectively. Y_2O_3-Al_2O_3 has been introduced into material B, which seems to have been effective in improving the bending strength and rolling fatigue strength.

Table 2. Experimental Results of Rolling Fatigue

Specimen Material	Load per Ball (N)	Experimental Number of Pieces	Life-to-Bearing Steel Ratio		Weibull Slope
			L_{10}	L_{50}	
Hot pressed materials					
SiC	196	15	0.0038	0.0039	1.82
ZrO_2	588	8	0.002	0.014	0.35
Si_3N_4 A	588	16	0.112	0.937	0.60
	1176	15	0.438	0.942	1.08
B	1176	14	1.8	4.2	1.01
Bearing steel	1928	24	1.0	1.0	1.88

2.2 Evaluation In Terms of Static Rated Load

Apart from the favorable evaluation of Si_3N_4 regarding its rolling fatigue strength, it is extremely important from a practical standpoint to confirm its static limit load. This can be easily called to mind since the static rated load of steel bearings has been defined by JIS [Japan Industrial Standards].

JIS defines the static limit load of steel bearings as "static load corresponding to the following calculated contact stress at the center of a contact area between the rolling element receiving the maximum load and the track," e.g., load corresponding to "4600 MPa with self-aligning ball bearings and 4200 MPa with other radial ball bearings."

The following is a description of an experiment involving a Si_3N_4 plate[2], which was conducted by the author's group as a preliminary test of the static rated load of ceramic bearings.

If a ceramic bearing is gradually loaded, unlike a steel one, Hertz cracks result under a certain load, which is deleterious to the ceramic bearings. To cope with this, the method shown in Figure 5 [not reproduced] has been developed for detecting the acoustic emission (AE) following crack initiation and finding the crack initiation load. Figure 6 [not reproduced] shows the cracks of the Si_3N_4 plate generated in the experiment, as well as the loads and total number of AE generated. The number of AE generated increases stepwise under loads Q_a and Q_b. On the other hand, two cracks were generated on the plate outside of a contact circle opposite loads Q_a and Q_b. Therefore, the crack initiation load can be measured from a load under which AE rapidly increases. Figure 7 [not reproduced] shows the crack initiation loads of Si_3N_4, indicating that these loads are significantly greater than the JIS values.

A study for determining the crack initiation loads of ceramic bearings by applying this method is under way[3),4)].

3. Study of Ceramic Bearing Application

3.1 Application to High Speed Conditions

A study applying ceramic bearings to high speed conditions has been conducted in the United States, with turbine bearings as its subject, since around 1976[5)-9)], with the DN value of a hybrid bearing with Si_3N_4 rolling elements incorporated into the inner and outer rings of a rolling bearing made from heat-resistant bearing steel reaching 2.5×10^6. The bearing is lubricated by a lube or grease. In the same year, a study to cope with the high speed needs of machine tools was initiated in Japan[10)-12)], resulting in the greatest progress in this field being made toward the commercial use of ceramic bearings. The following is an example of basic research on its commercial use[11)]. Figure 8

[not reproduced] shows the measured results of the outer ring temperature when the spindle is operated by oil air lubrication for high speed machining. It is found that the use of an Si_3N_4 ball has enabled the bearing temperature to be controlled low. The bearing using a steel ball has caused a rapid rise in temperature and wear at 18,000 rpm, while the hybrid bearing normally rotates at up to 24,000 rpm (DN value of 1.56×10^6).

The dominance of a hybrid bearing lies in the fact that the centrifugal force and gyro moment can be minimized, that the contact surface pressure resulting from the thermal expansion difference can be relaxed, and that seizure rarely occurs due to chemical stability of ceramics seizure. A study applying a ceramic bearing to the main shafts of a jet engine[13),14)] has recently been started in Japan.

3.2 Application to High Temperature Conditions

High temperature areas are the most suitable field for utilizing such characteristics of a ceramic bearing as heat resistance and chemical stability (seizure resistance). However, its application in this field has not yet been achieved, for which the lack of availability of a lubricant suitable for use at high temperatures is most responsible. The development of solid lubricants usable in a wide temperature range of up to 1,000°C[15)-21)] is making progress. These results will be applied to high temperature bearings in the future.

Referring now to the experiment by the author and his group involving a ceramic bearing incorporating a high temperature solid lubricant retainer[22)], Figure 9 [not reproduced] illustrates an experimental device for evaluating the operating performance of ceramic bearings at high temperatures. The tested bearing is an angular ball bearing with an inner diameter of 20 mm. The operating performance is evaluated by measuring friction torque and vibration. Friction torque and vibration indicate the lubricity of solid lubricants and their adherent quality, respectively. As long as lubrication by a method utilizing this quality is applied, the wear of a retainer material directly controls the life of a bearing, thus becoming a factor of the evaluation. The experiment was conducted under the following conditions: temperature, 500°C, rotating speed, 1,000 to 15,000 rpm; axial load, 40 kgf. The tested bearing is of a transverse assembly.

Figures 10 and 11 [not reproduced] show examples of experimental results. The symbols in the drawings are as shown in Table 3. It has been found that Sb impregnated graphite (C-Sb-I) is low in friction torque with stable vibration. C-Sb-I was also superior with respect to wear.

Table 3. Retainer Materials

	C-Sb-I	C-Sb-II	C-Sb-III
Matrix graphite	1G11	1G11	ISO88
Impregnated metal	Antimony	Antimony/tin alloy	Antimony
Mixing ratio	-	6:4	-
Impregnation amount	47	47	47

3.3 Miscellaneous

Ceramic bearings are increasingly being applied to such fields as chemicals and water-related industries which involve a corrosive atmosphere for steel bearings[23)-25)]. Reference 24 describes the development of an excellent ceramic material introducing CeO_2-MgO for a sintering assistant, superior not only in corrosion resistance but also in rolling fatigue strength. It has also been reported that the practical use of ceramic bearings has been achieved in their applications requiring corrosion resistance, such as surface treatment tanks for steel plates. Their application to vacuums is being attempted[26)].

4. Conclusion

The outline of the current status of studies on the application of ceramics to rolling bearings has been described based on references.

Hampering an increase in the demand for ceramic bearings, despite the expectations for them, seems to include high cost, insufficient reliability, a problem of lubrication at high temperatures and limited applications. It has been forecast that the price of a ceramic ball in 1992 will be reduced to below one-fifth that in 1987[27)]. It is important to make clear the availability and reliability of ceramic bearings and, since the cost depends on production, further research to this end is expected.

References

1. Kikuchi, K., et al., LUBRICATION, Vol 28 No 6, 1983 p 465.

2. Fujihara, t., et al., LUBRICATION, Vol 33 No 4, 1988 p 461.

3. Yoshioka, T., et al., MATERIAL TESTING TECHNOLOGY, Vol 36 No 4, 1991 p 461.

4. Nakada, et al., PREPRINTS OF THE TRIBOLOGY CONFERENCE, JAPAN LUBRICATION SOCIETY, No 5, 1991 p 237.

5. Bhushan, B., Sibley, L.B., ASLE TRANS, Vol 25 No 4, 1982 p 417.

6. Reddecliff, J.M., Valori, R., ASME TRANS, Vol 98 No 4, 1976 p 553.

7. Bersch, C.F., Weinberg, P., "SAE Paper No 790108."

8. Hambug, G., Cowley, P., Valori, R., ASLE Preprint 80-AM-3C-1.

9. Miner, J.R., Grace, W.A., Valori, R., ASLE Preprint 80-AM-3C-3.

10. Ohmori, T., et al., NTN TECHNICAL REVIEW, Vol 56, 1988 p 46.

11. Shoda, Y., NSK TECHNICAL JOURNAL, No 650, 1989 p 21.

12. Ichikawa, Y., KOYO ENGINEERING JOURNAL, Vol 135, 1989 p 62.

13. Seki, K., PREPRINTS OF THE TRIBOLOGY CONFERENCE, JAPAN LUBRICATION SOCIETY, Vol 1991-10, 1991 p 75.

14. Taki, M., PROCEEDINGS OF THE 69TH NATIONAL CONFERENCE, JAPAN MACHINERY SOCIETY, 910-62, Vol C, 1991 p 458.

15. Umeda, K., et al., PREPRINTS OF THE JAPAN TRIBOLOGY SOCIETY CONFERENCE, 1991-5, 1991 p 9.

16. Umeda, K., et al., PREPRINTS OF THE MECHANICAL ENGINEERING LABORATORY WORKSHOP, 1991-3, 1991.

17. Enomoto, Y., et al., CHEMISTRY AND INDUSTRY, Vol 44 No 5, 1991 p 818.

18. Umeda, K., et al., LUBRICATION, Vol 33 No 1, 1988 p 54.

19. Sliney, H.E., TRIBOLOGY INTERNATIONAL, Vol 15 No 5, 1982 p 303.

20. Allam, I.M., JOURNAL OF MATERIALS SCIENCE, Vol 26, 1991 p 3977.

21. Wedeven, L.D., Pallini, R.A., Aggarwal, B.B., PROC 23RD AUTOMOT TECHNOL DEV CONTACT COORD MEET, 1986 p 99.

22. Koizumi, S., et al., PREPRINTS OF THE 34TH NATIONAL CONFERENCE, JAPAN LUBRICATION SOCIETY, 1989 p 589.

23. Knoch, H., MATERIALS AUSTRALASIA, Vol 21 No 2, 1989 p 6.

24. Nizeki, S., et al., PREPRINTS OF THE JAPAN LUBRICATION SOCIETY TRIBOLOGY CONFERENCE, 1991-10, p 67.

25. Minami, M., et al., PREPRINTS OF THE JAPAN LUBRICATION SOCIETY TRIBOLOGY CONFERENCE, 1991-10, p 107.

26. Seki, K., et al., PREPRINTS OF THE JAPAN LUBRICATION SOCIETY TRIBOLOGY CONFERENCE, 1991-10, p 71.

27. Chudecki, J.F., SAE TECHNICAL PAPER SERIES, 891904.

Tribology of Ceramics Engine

926C0070G Tokyo DAI 12-KAI SENTAN GIJUTSU FORAMU in Japanese 14 Feb 92 pp 46-51

[Article by H. Kawamura, Isuzu Ceramics Research Institute]

[Text]

1. Introduction

The development of a thermal insulating ceramic engine, which was begun in the 1980s and was dealt with by most engine research institutes, at one time experienced significant growth. Currently, however, its development is only being promoted by a few research institutes, with many researchers having given up its development. An analysis of conventional research into the development of a thermally insulated engine finds that the basic studies of too many developmental items, such as ceramic materials, engine structure, high temperature combustion, etc., have not been sufficient. This is true of ceramics tribology, making it necessary to study which characteristics are required for engine materials. This article will describe the tribology of ceramics for utilization as engine materials.

2. Structure of Thermally Insulated Engine

A thermally insulated engine is one whose combustion chamber, where fuel used to be burned, is composed of heat-resistant materials, such as ceramics, while cooling takes place around it with water or air, intending to remove the cooling unit from the engine itself. In an engine with such a structure, the temperature of the cylinder liner increases remarkably, making it impossible for pistons to slide, which is the basic operation of a reciprocating engine. The temperature at the piston sliding area exceeds 400°C, thereby disabling normal lubrication from being performed. Although a study of solid lubricants is being made so as to enable pistons to slide at high temperatures to cope with this, low friction coefficients have not yet been obtained.

The author and his group have changed the engine structure so as to make the temperature of the cylinder liner optimum to enable sliding operations between the piston and the cylinder to occur with a minimum frictional force. In other words, the cylinder liner is divided into upper and lower parts so that the heat of the former does not transfer to the latter, and the piston is divided in the same manner so that the heat received by the upper surface does not transfer to the piston ring. The temperature of the cylinder liner with such a structure drops to below 200°C, which is the optimum temperature for lubricated piston sliding. Figure 3 [not reproduced] illustrates the structure of a thermal insulating engine, with Figure 4 [not reproduced] showing the temperature distribution of a cylinder liner.

3. Friction of Ceramic Materials

Two frictional forces involving boundary lubrication and fluid lubrication act between the piston ring and cylinder liner of an engine in reciprocating motion. Boundary lubrication occurs when the piston reaches the neighborhood of the upper dead point, resulting in zero velocity with the piston ring pressed against the cylinder side under the cylinder's pressure. Fluid lubrication acts in other areas, with the frictional force depending on the viscosity of the lubricant.

To lessen the frictional force in boundary lubrication, a fluid must exist between the sliding solids and there must be a chemical adsorption film to withstand the local pressure. With the chemical reactivity between the molecules contained in ceramics and the lubricant seeming to be an important factor for the formation of a chemical

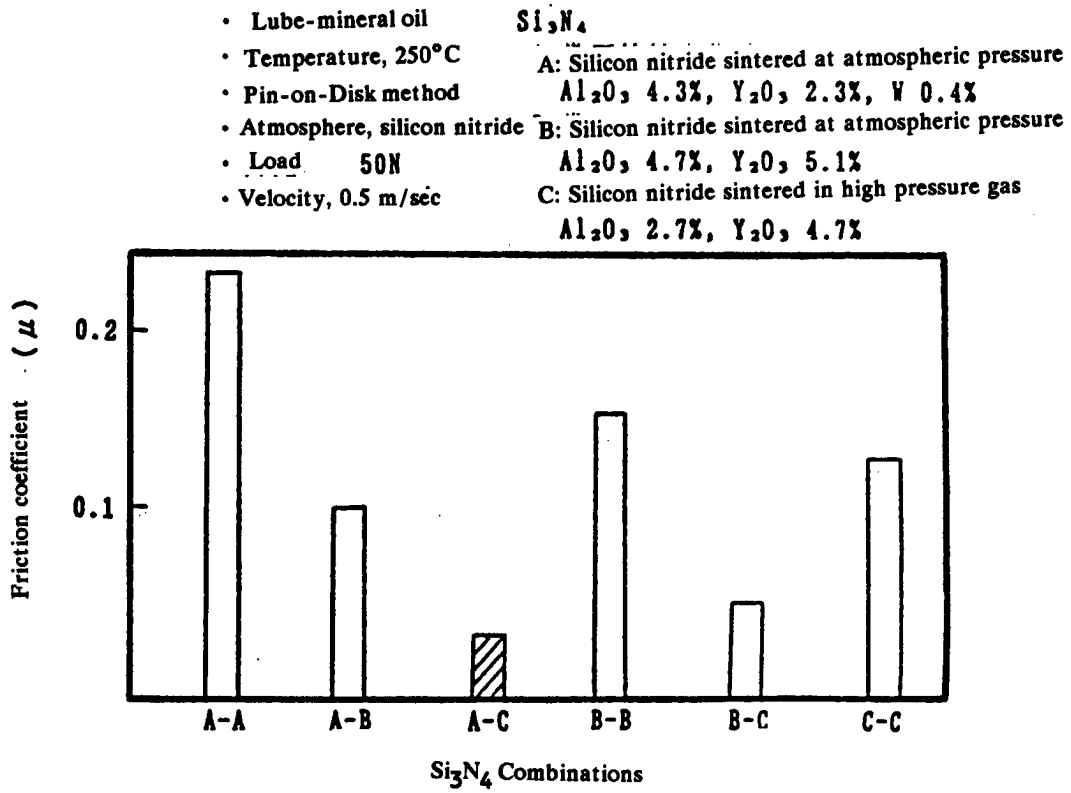

Figure 6. Friction Coefficients of Combined Silicon Nitrides in Boundary Lubrication

adsorption film, various ceramics with different components were prepared, which were combined by the Pin-on-Disk method, and their friction coefficients were examined under boundary lubrication conditions. The results are shown in Figure 5 [not reproduced]. These test results have found that a combination of silicon nitrides of different kinds enables friction coefficients to be lessened. In this context, silicon nitrides with different additives were collected for a friction test. Figure 6 shows the results. Figure 7 [not reproduced] shows the microtissues of silicon nitrides with small friction coefficients as observed by a transmission electron microscope. In silicon nitride sintered at atmospheric pressure, multiple vitreous layers containing alumina, yttria, etc., exist around the crystals and pores are observed among crystal particles, while in silicon nitrides sintered at high pressure, only thin vitreous layers exist around the crystals which have developed in needle form, with the pores being extremely small. Small friction coefficients could be obtained only when these two materials were combined, thereby suggesting that the factor for lessening the friction coefficients in boundary lubrication existed in this fact. Components contained in silicon nitrides seeming to affect the production of adsorption films and the friction coefficients of silicon nitrides sintered at atmospheric pressure were examined. The results are shown in Figure 8. A combination of silicon nitride sintered at atmospheric pressure, and particularly one containing a large amount of yttria and silicon nitride sintered at gas pressure with close tissues, has provided the lowest friction coefficient, which seems to represent the factor for yttria producing an adsorption film.

In order to lessen the friction coefficients in ceramics-ceramics boundary lubrication, soft metallic components are made to adhere to the surface of silicon nitride, and the effect of a physical adsorption film on relaxing a shear force during sliding operations was also examined. As specimens, MoDTP and ZnDTP were mixed with a lube for a friction test. Figure 9 shows the test results. Friction coefficients did not lessen very much, but rather became equivalent to the value of the metal. Thus, it has been found that in order to reduce the friction coefficients of silicon nitride, it is important to evaluate the production of the chemical adsorption film by the components contained in its tissues and a lube.

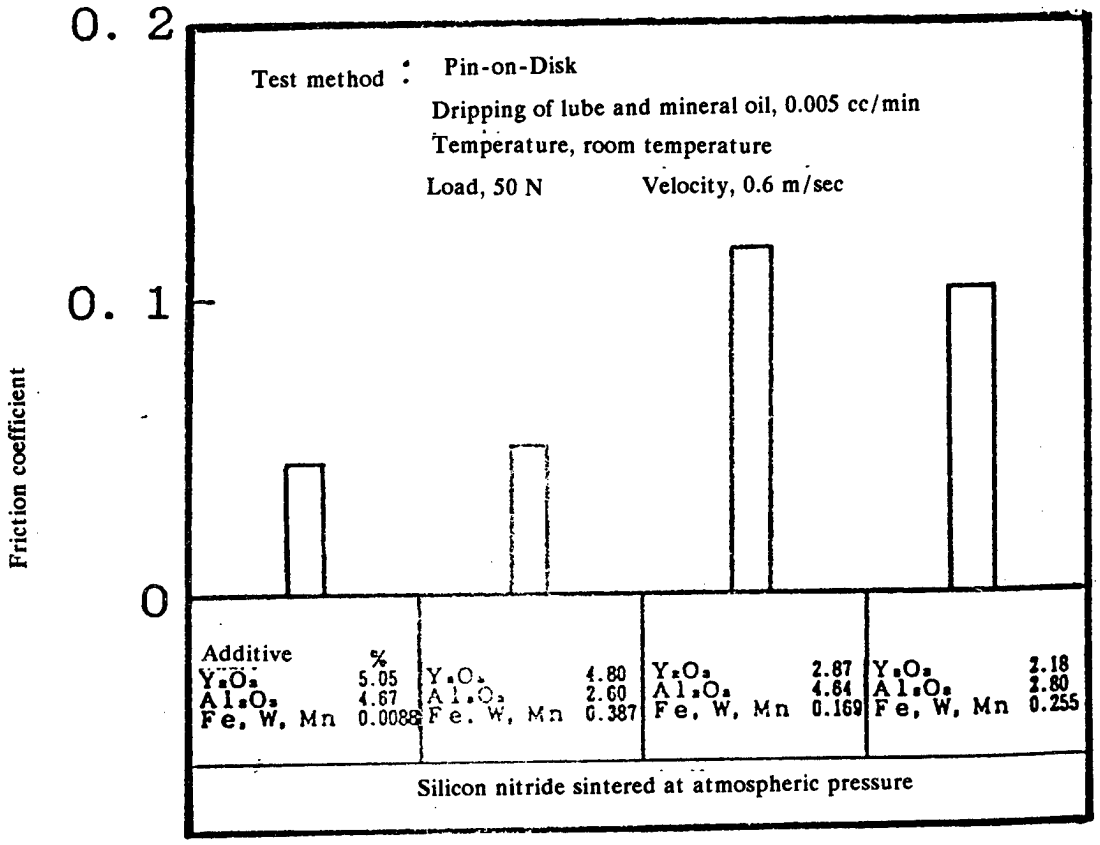

Figure 8. Friction Coefficients of Silicon Nitride Sintered at Atmospheric Pressure Combined with Silicon Nitride Sintered at Gas Pressure

4. Ceramic Solid Lubricant and Friction

Research into two-cycle engines has recently made progress, although lubrication has always posed problems in their development. In other words, with a port to accept the intake air existing at the bottom of the cylinder, a lube flowing into the port during the vertical motion of the cylinder fails to burn completely in the combusion chamber, and is discharged as hydrocarbon (HC). This HC can only be reduced by not using a lube, and solid lubricants meet the requirement. CaF_2 was applied to the surface of the silicon nitride to examine its friction coefficient. The friction coefficient decreased to 0.2 with a rise in temperature. Its sliding surface was examined, finding that a $Ca_8Si_5O_{18}$ or Ca_2SiO_4 film was produced, suggesting that this film can shift according to the action of frictional force. This film seems to adhere stably to the surface as it reacts with silicon nitride. For this reason, no abrasion loss was observed in a friction test exceeding 1,000 hours, proving that the film serves as a solid lubricant. Figures 10 and 11 show the results of the friction test and the results of observation of the existence of a reaction layer with Si inside the silicon nitride used for the friction test, respectively. Figure 12 [not reproduced] shows the observed results of a Ca-Si-O film formed on the surface.

5. Conclusion

Ceramic materials, strong in covalent bond quality and posing no fear of coagulating at high temperatures, are convenient for use in ceramic engines operating at high temperatures. With their friction coefficients minimizable under the influence of material additives, it is possible for ceramics to be used as engine members, thereby reducing the frictional force of the engines. Furthermore, the lubrication of two-cycle engines will very likely be improved with the utilization of solid lubricants, etc., thus necessitating their promotion in studying ceramics as sliding materials.

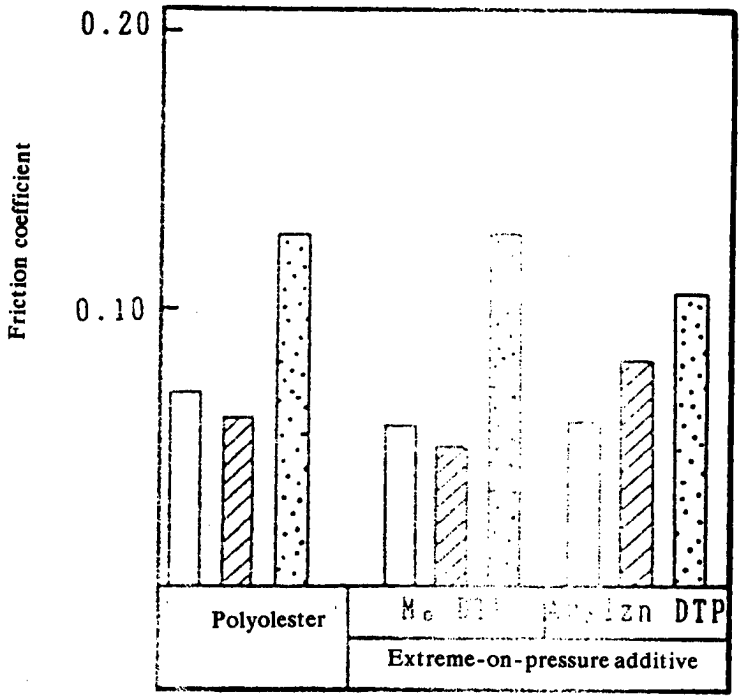

Test method: Pin-on-Disk

Velocity: 0.6 m/sec

Load: 50 N

Lube: dripping by 0.005 cc/min

Materials sintered at atmospheric pressure and gas pressure

Gas pressure sintered material combination

Steel-steel combination

Figure 9. Effect of Physical Adsorption Film on Friction Coefficients

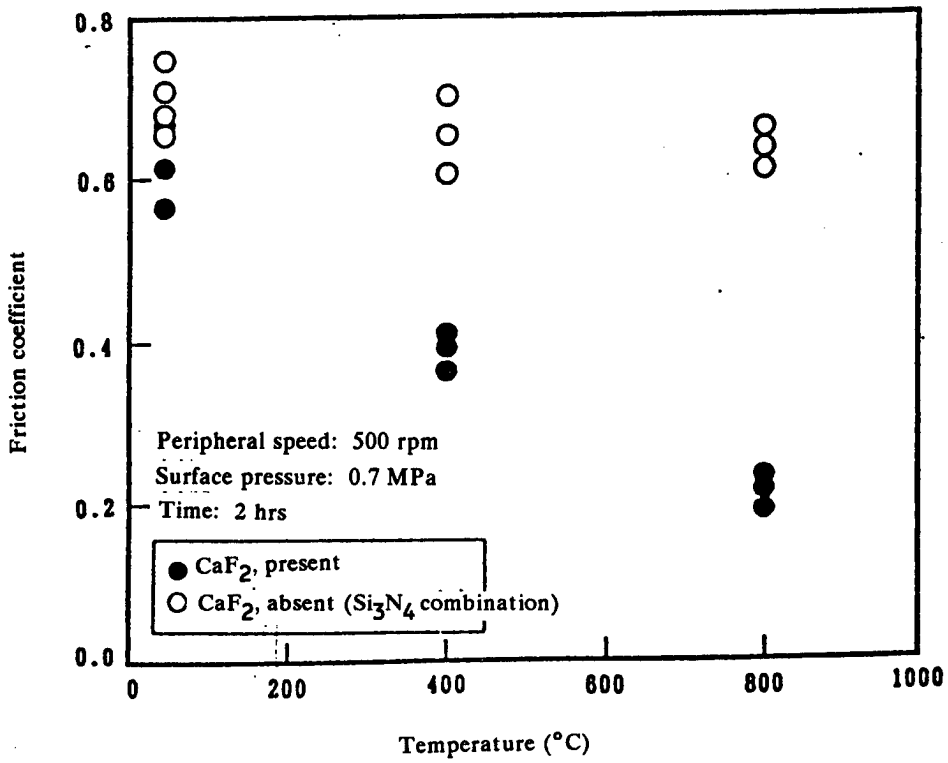

Figure 10. Friction Coefficients at Respective Temperatures

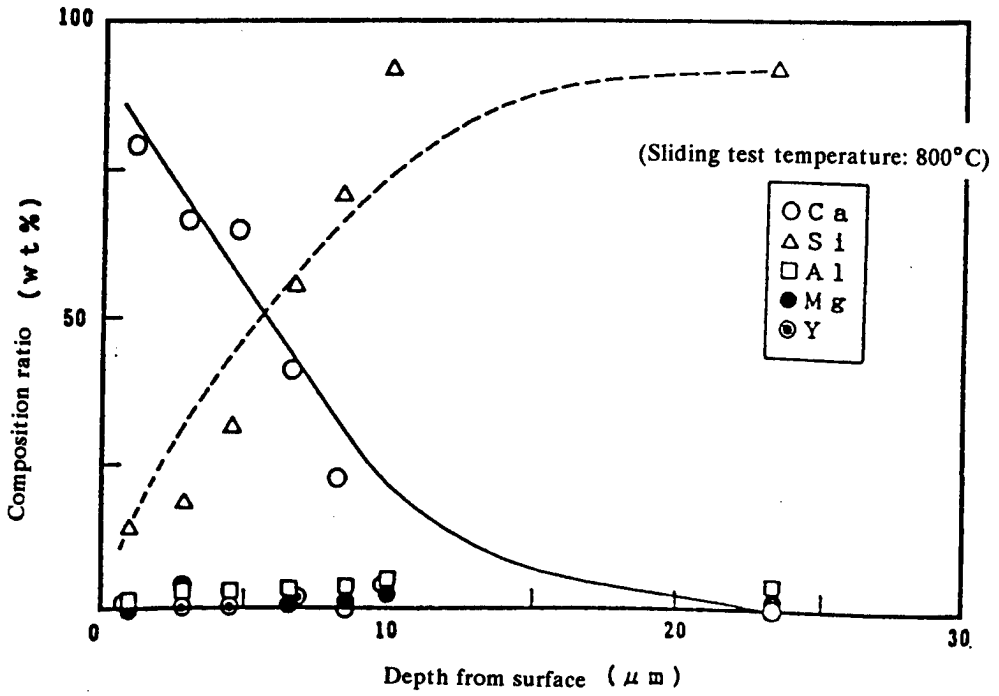

Figure 11. Results of EDX Analysis on Depth Direction of Sliding Surface

Ceramic Applications to Gas Turbines

926C0070H Tokyo DAI 12-KAI SENTAN GIJUTSU FORAMU in Japanese 14 Feb 92 pp 52-57

[Article by T. Itoh, Japan Automobile Research Institute]

[Text]

1. Introduction

In Japan, where oil energy resources are scarce, the advent of automobile engines capable of using various fuels without being limited by the octane or cetane rating, yet demonstrating high thermal efficiency and being clean with respect to exhaust release, are eagerly anticipated for the stable supply and effective utilization of energy resources, with a ceramic gas turbine considered to represent one of the most promising candidates. Under such circumstances, the "Development of the Automobile Ceramic Gas Turbine" project was initiated at the Oil Industry Activation Center in June 1991 as auxiliary work by the Agency of Natural Resources and Energy, MITI, with the active cooperation of related industries, such as oil, automobiles and ceramics.

Western countries have also tackled similar national projects for the past 10-odd years but have been unable to complete an automotive engine, and a number of problems, led by ceramic application technology, remaining unsolved. This article will outline the developmental technical problems, their feasibilities and upcoming schedules, focusing on the above-mentioned "Development of the Automobile Ceramic Gas Turbine."

2. Basic R&D Plan

2.1 Developmental Target

The future trends of automobiles and automotive engines have been examined and forecast, with the result that it has been judged that "thermal efficiency," "exhaust characteristics" and "multi-fuel quality" are particularly important, in addition to the general characteristics for automobile-use engines, with the final achievement target shown in Table 1 [not reproduced] having been set.

2.2 Technical Problems of Ceramic Gas Turbine

When technical problems are summarized by making reference to the R&D developmental processes carried out to date in Japan and the foregoing American AGT and ATTAP projects, they can be divided into the following four fields: improved performance of miniature gas turbine elements (compressor and turbine), improvement of low Nox fuel technology, improvement of heat exchange and thermal insulation technology, and improvement of ceramics application technology. Of these, in addition to the problems with materials and

manufacturing technology, the ceramics application technology directly related to this forum involves the following as concrete problems:

(1) Large ceramic parts are difficult to make and provide low reliability, and it is also hard to prevent air and gas from leaking out of combined small part clearances—interpart leakage preventive structure;

(2) Not all parts can be made of ceramics. It is difficult to achieve interfaces with metallic portions in the high temperature area (how to cope with deformation and thermal expansion differences)—junction between the ceramic rotor and metallic shaft, a method for supporting ceramic stationary parts to the metallic housing and head exchanger seal structure;

(3) The high temperature nonlubrication area lacks durability—a seal sliding material for the heat exchanger;

(4) Damage may be caused by microparticle collisions (FOD)—turbine rotors and nozzles.

To solve these problems, it is indispensable that the process of design, manufacturing, experimentation and analysis be repeated over and over in order to accumulate techniques in every aspect. The project will be implemented through a seven-year program.

2.3 Development Schedule

Prior to the development of an engine, it is necessary to raise the levels of key technologies. The scheduled seven years have roughly been divided into two, i.e., three years in the first term (FY 1990 to 1992) and four years in the latter term (FY 1993 to 1996). In the former, mainly key technologies will be developed, while the latter will mainly involve the development of an engine. Figure 1 outlines the seven-year development program.

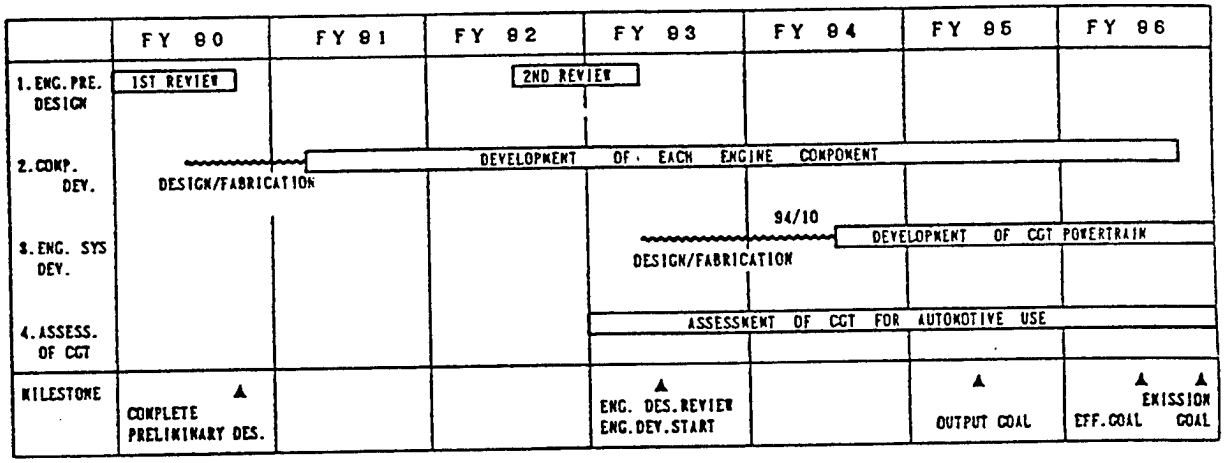

Figure 1. Outline of Developmental Schedule

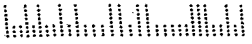

Foreign Broadcast Information Service (FBIS) and Joint Publications Research Service (JPRS) publications contain political, military, economic, environmental, and sociological news, commentary, and other information, as well as scientific and technical data and reports. All information has been obtained from foreign radio and television broadcasts, news agency transmissions, newspapers, books, and periodicals. Items generally are processed from the first or best available sources. It should not be inferred that they have been disseminated only in the medium, in the language, or to the area indicated. Items from foreign language sources are translated; those from English-language sources are transcribed. Except for excluding certain diacritics, FBIS renders personal names and place-names in accordance with the romanization systems approved for U.S. Government publications by the U.S. Board of Geographic Names.

Headlines, editorial reports, and material enclosed in brackets [ ] are supplied by FBIS/JPRS. Processing indicators such as [Text] or [Excerpts] in the first line of each item indicate how the information was processed from the original. Unfamiliar names rendered phonetically are enclosed in parentheses. Words or names preceded by a question mark and enclosed in parentheses were not clear from the original source but have been supplied as appropriate to the context. Other unattributed parenthetical notes within the body of an item originate with the source. Times within items are as given by the source. Passages in boldface or italics are as published.

SUBSCRIPTION/PROCUREMENT INFORMATION

The FBIS DAILY REPORT contains current news and information and is published Monday through Friday in eight volumes: China, East Europe, Central Eurasia, East Asia, Near East & South Asia, Sub-Saharan Africa, Latin America, and West Europe. Supplements to the DAILY REPORTs may also be available periodically and will be distributed to regular DAILY REPORT subscribers. JPRS publications, which include approximately 50 regional, worldwide, and topical reports, generally contain less time-sensitive information and are published periodically.

Current DAILY REPORTs and JPRS publications are listed in *Government Reports Announcements* issued semimonthly by the National Technical Information Service (NTIS), 5285 Port Royal Road, Springfield, Virginia 22161 and the *Monthly Catalog of U.S. Government Publications* issued by the Superintendent of Documents, U.S. Government Printing Office, Washington, D.C. 20402.

The public may subscribe to either hardcover or microfiche versions of the DAILY REPORTs and JPRS publications through NTIS at the above address or by calling (703) 487-4630. Subscription rates will be provided by NTIS upon request. Subscriptions are available outside the United States from NTIS or appointed foreign dealers. New subscribers should expect a 30-day delay in receipt of the first issue.

U.S. Government offices may obtain subscriptions to the DAILY REPORTs or JPRS publications (hardcover or microfiche) at no charge through their sponsoring organizations. For additional information or assistance, call FBIS, (202) 338-6735,or write to P.O. Box 2604, Washington, D.C. 20013. Department of Defense consumers are required to submit requests through appropriate command validation channels to DIA, RTS-2C, Washington, D.C. 20301. (Telephone: (202) 373-3771, Autovon: 243-3771.)

Back issues or single copies of the DAILY REPORTs and JPRS publications are not available. Both the DAILY REPORTs and the JPRS publications are on file for public reference at the Library of Congress and at many Federal Depository Libraries. Reference copies may also be seen at many public and university libraries throughout the United States.